

Rayleigh Lecture 2012

Jet Noise Prediction: A Historical Perspective and Future Directions



Philip J. Morris

Boeing/A.D. Welliver Professor

Department of Aerospace Engineering

Penn State University

Internoise 2012

August 19-23, 2012

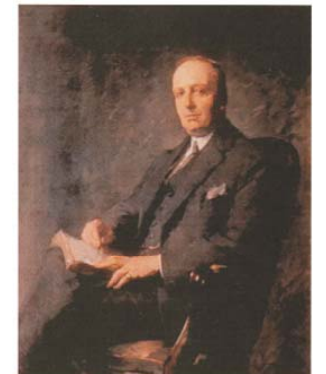
New York, NY

Outline

- Rayleigh and the Rayleigh Lecture
- The jet noise problem
- Jet noise observations
- Jet noise prediction
 - Acoustic analogies
 - Noise from large scale turbulence
 - Computational approaches
- Jet noise reduction
- Future directions

Family History

- John Strutt MP (1727-1816)
 - Bought Terling Place, 1761
- Joseph Holden Strutt (1758-1845)
 - MP and Colonel in West Essex Regiment
 - Declined peerage in favor of his wife (1st Baroness Rayleigh)
- John James Strutt (1796-1873)
 - Second Baron Rayleigh
- John William Strutt (1842-1919)
 - Married Evelyn Balfour (1871)
 - 3rd Baron Rayleigh (1873)
- Robert John Strutt (1875-1947)
 - 4th Baron Rayleigh (Rayleigh: unit of luminosity)



Lord Rayleigh (John William Strutt)

- 1842 – 1919
- Eton (1853), Wimbledon (1854-56), Harrow (1857) and Highstead, Torquay(1857-61)
- Cambridge 1861 – 1871
 - Taught by Stokes, Routh
 - Senior Wrangler (1864)
- Lord Rayleigh in 1873 (Third Baron Rayleigh)
- Nobel Prize for Physics in 1904 (Discovery of Argon)



Terling Place



Terling Place Laboratory



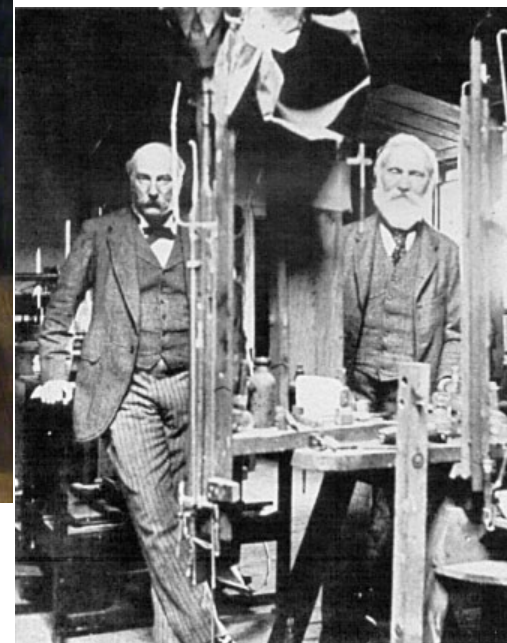
The west wing



One of the main laboratories



Rayleigh in his laboratory:
Edward Burne-Jones (1921)



Rayleigh and Kelvin (1904)

Some Achievements

- Rayleigh distribution – Statistics
- Rayleigh-Jeans law – Black-body radiation
- Rayleigh scattering – Color of sky
- Rayleigh damping – Vibrations
- Rayleigh quotient – Eigenvalue algorithms
- Rayleigh-Ritz method – mechanical resonances
- Rayleigh disc – Air particle velocity
- Rayleigh waves – Surface waves
- Rayleigh fading – electromagnetic propagation
- Rayleigh criterion – Optical resolution
- Rayleigh instability criterion – inviscid instability
- Rayleigh criterion – combustion instability
- Rayleigh interferometer – Refractometry
- Rayleigh number – Turbulence
- Rayleigh-Taylor instability – Immiscible fluids
- Rayleigh-Plesset equation – Bubble dynamics
- Rayleigh streaming: nonlinear acoustics
- Rayleigh-Schrödinger HFPT – Perturbation theory
- Rayleigh-Born approximation – Scattering theory



Rayleigh conductivity

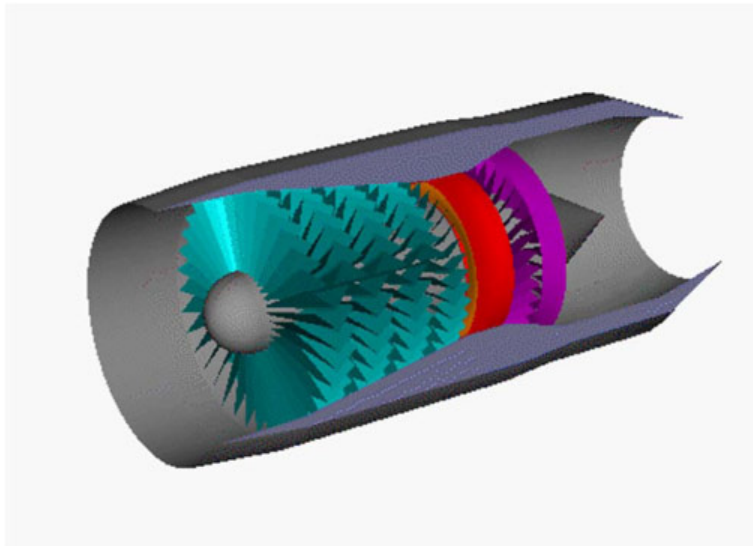
References

- “Life of Lord Rayleigh,” Robert J. Strutt, 1968
- “Lord Rayleigh: the Man and his Work,” R. Bruce Lindsay, 1970
- “John William Strutt: Victorian Polymath,” Institute of Physics, 2009
- “Lord Rayleigh,” Peter Wells, IEEE Ultrasonics Symposium, 2005.
- “Lord Rayleigh,” Peter Wells, NPL Lecture, recorded Oct. 2007, Youtube
- “Lord Rayleigh: A master of theory and experiment in acoustics,” D. M. Campbell, Acoust. Sci & Tech., 28(4) 2007.

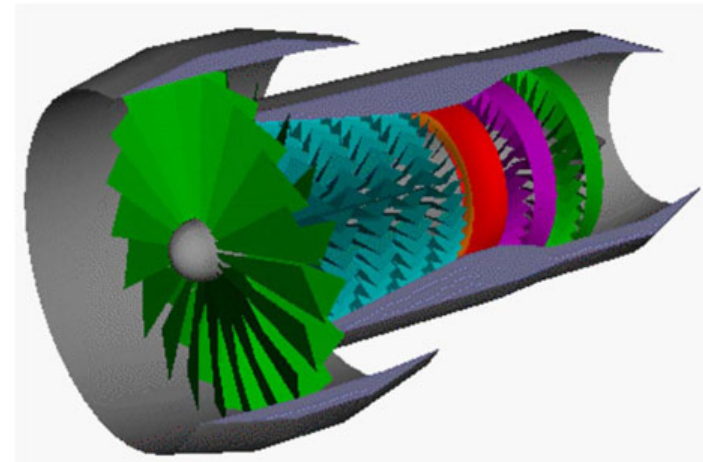
Rayleigh Lecture

- ASME: Noise Control and Acoustics Division
- Established 1985
- This award is given in recognition of presenting the Rayleigh Lecture at the annual ASME International Mechanical Engineering Congress and Exposition. Lecturers are selected among those who have made pioneering contributions to the sciences and applications of noise control and acoustics
- Previous lecturers: Ffowcs Williams, Powell, Lighthill, Blackstock, Pierce, Crighton, Howe, Koopman, Blake, Willaims, Atassi, Thompson, Schlinker,...

Jet Engines and Noise



Basic Turbojet Engine

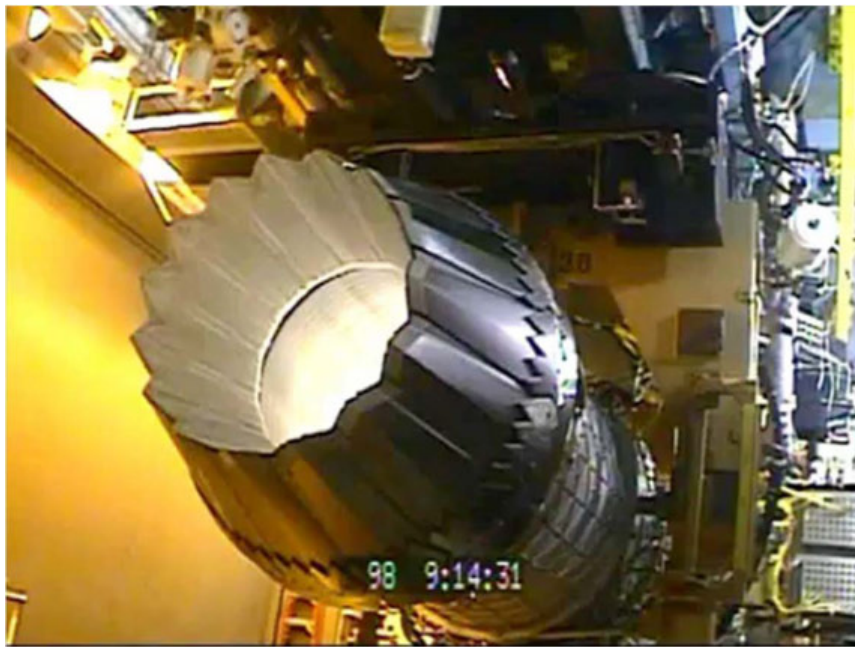


Basic Turbofan Engine

Courtesy: NASA Glenn RC

Turbofan Engines

Low Bypass Ratio



Pratt & Whitney F135

High Bypass Ratio



General Electric GENx

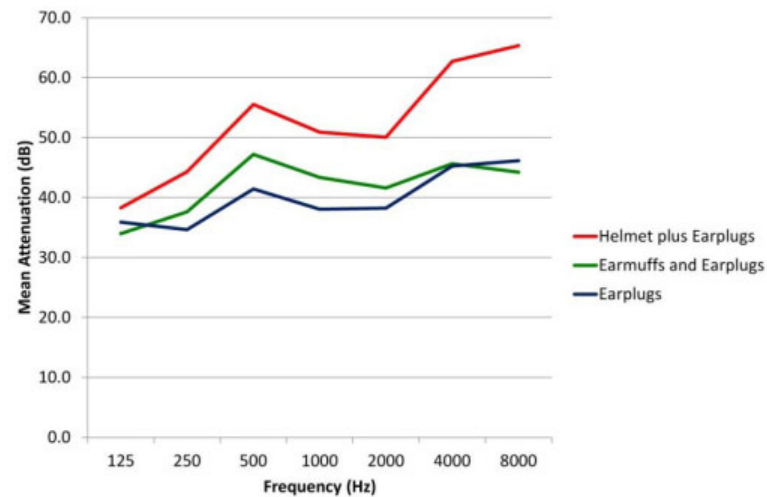
Navy Personnel



Landing Safety Officers

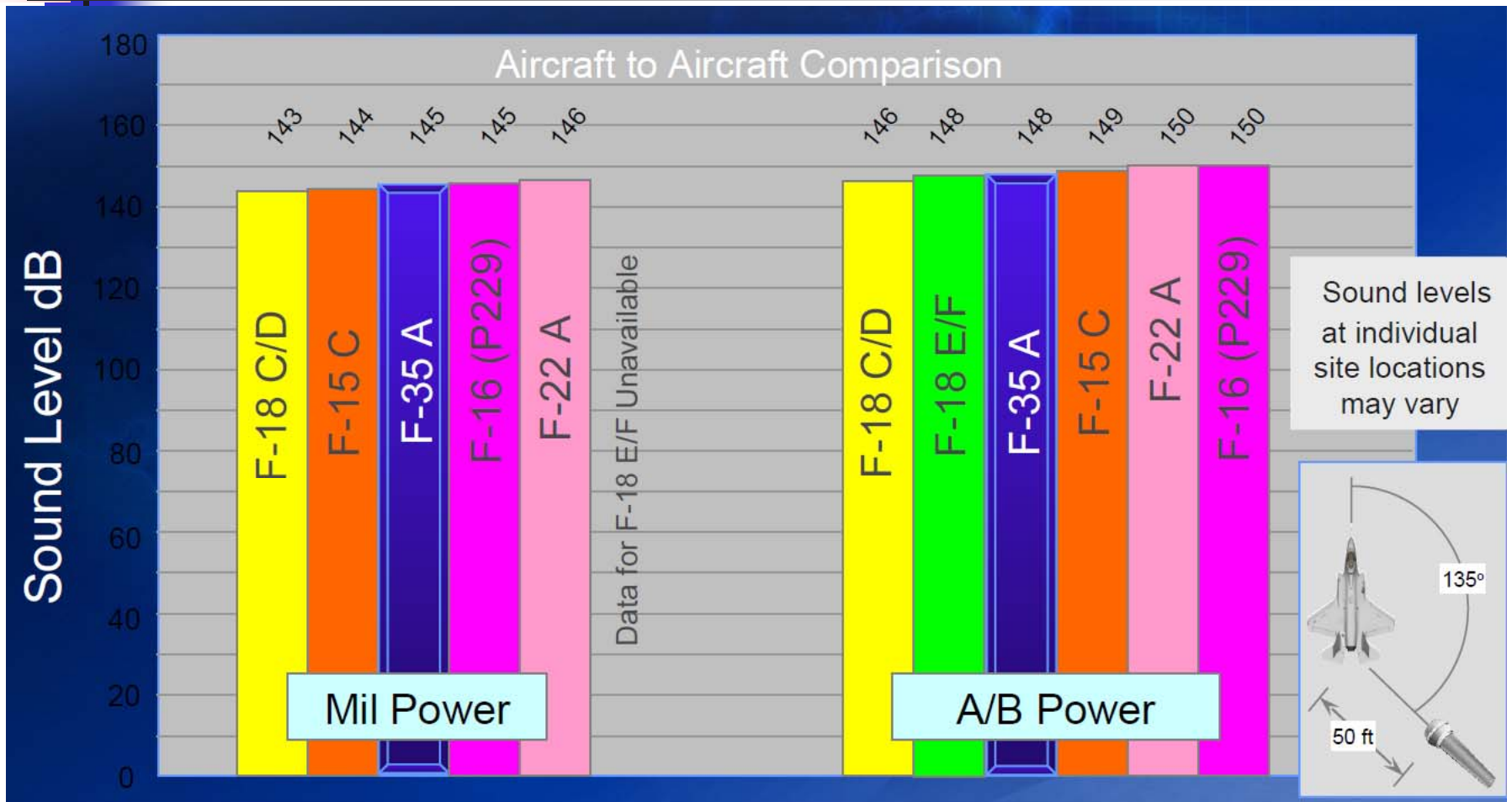


Hearing Protection



Dietz et al. (2011)

Jet Noise Levels



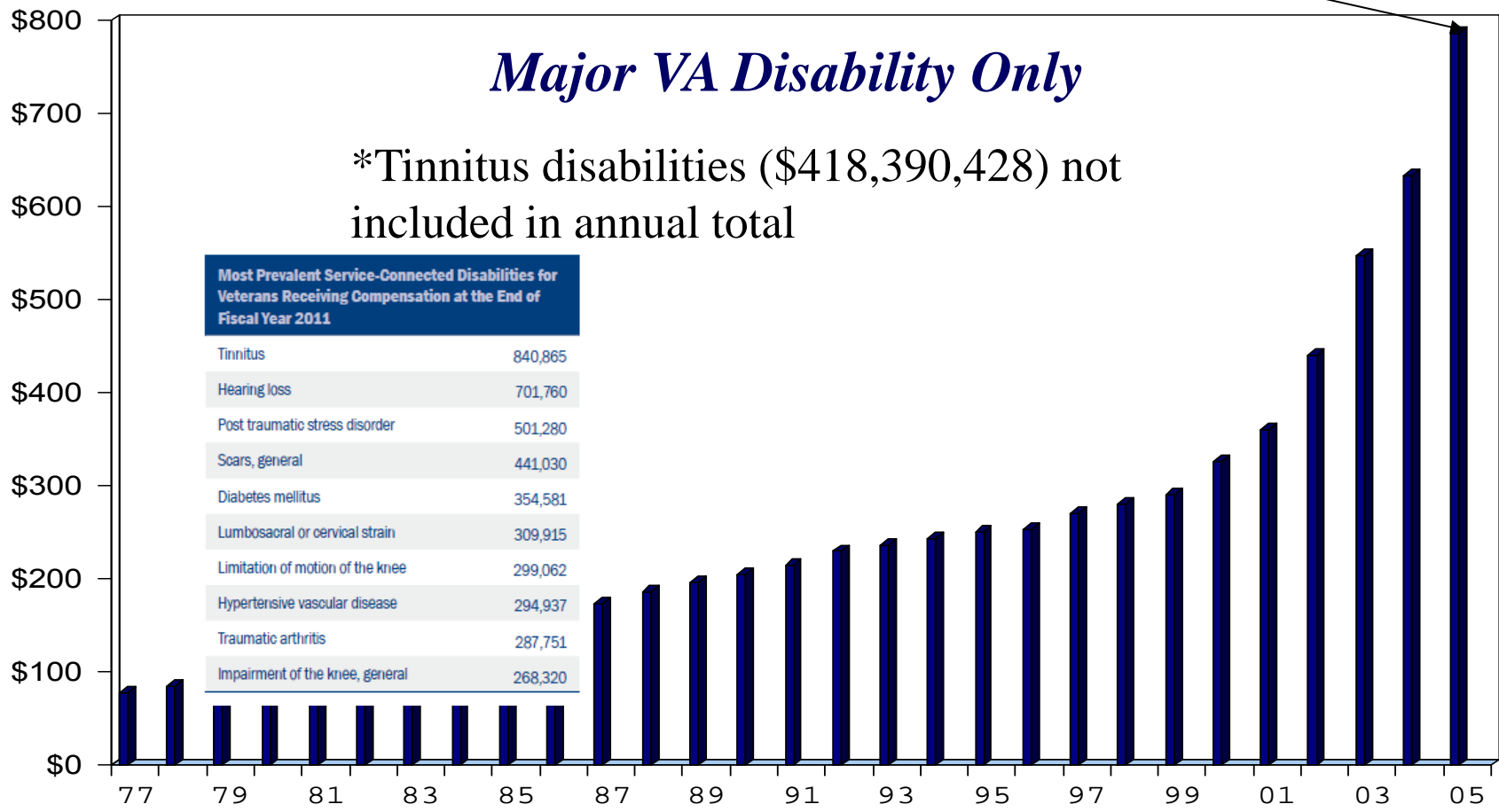
Near-Field F-35 Sound Levels Are Comparable to Current Fighter Aircraft

Cost of Hearing Loss for All Veterans 1977-2005

Total = \$7,484,419,681

Millions

\$786,048,420*



Veterans Benefits Administration (2011)



Jet Noise Observations

- Overall Characteristics
 - Noise mechanisms
- Velocity Dependence
 - Effect of temperature and observer angle
- Theory and Prediction Methods

Flow Properties

- Unsteady visualizations

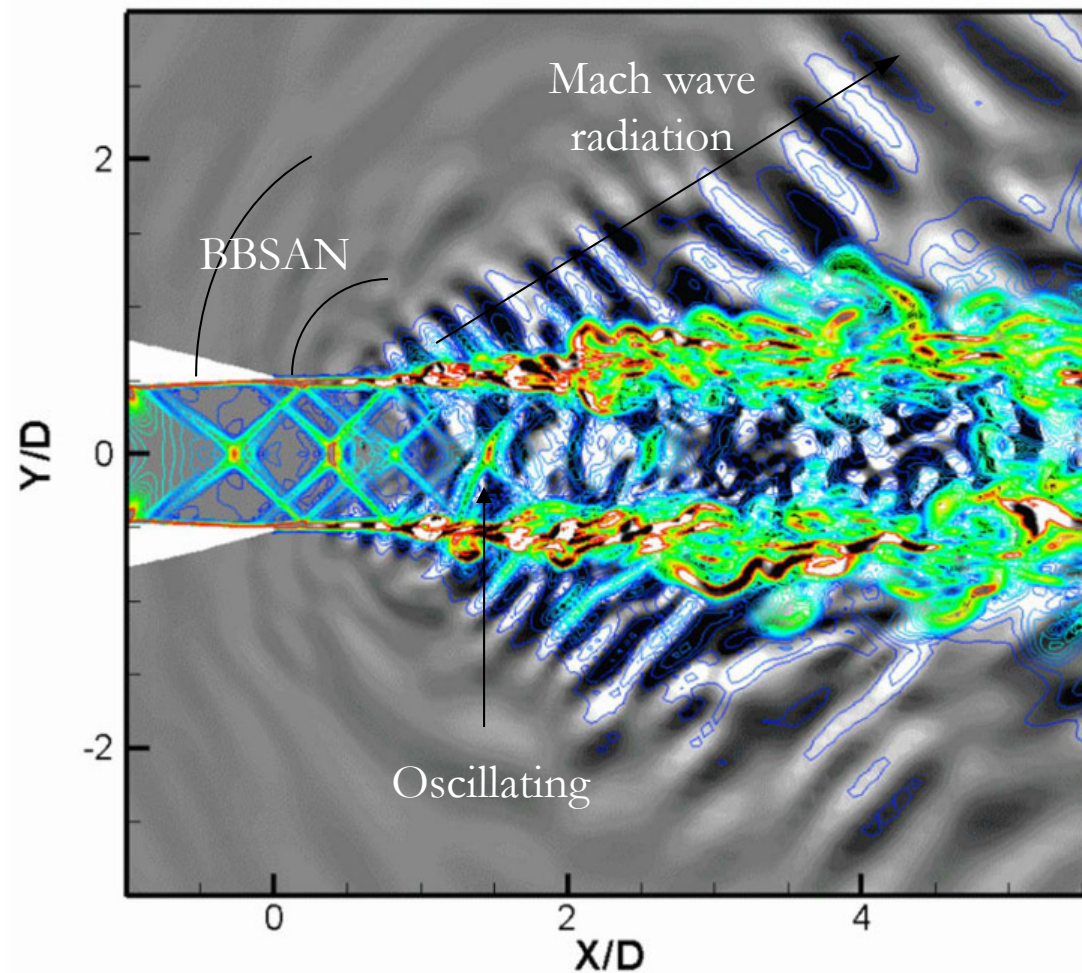
Color contours

Density gradient

Gray background

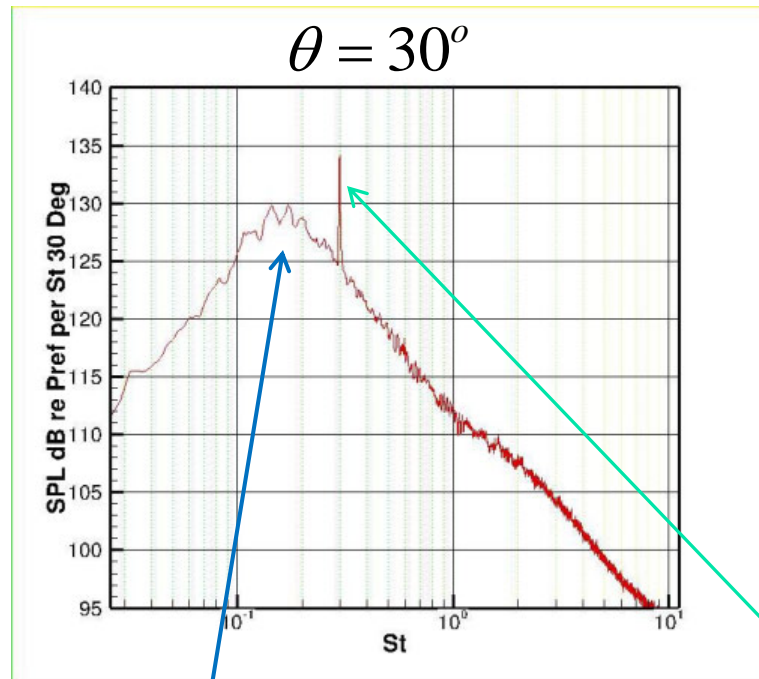
Pressure time-
derivative

Baseline, $M_j=1.47$
Animation

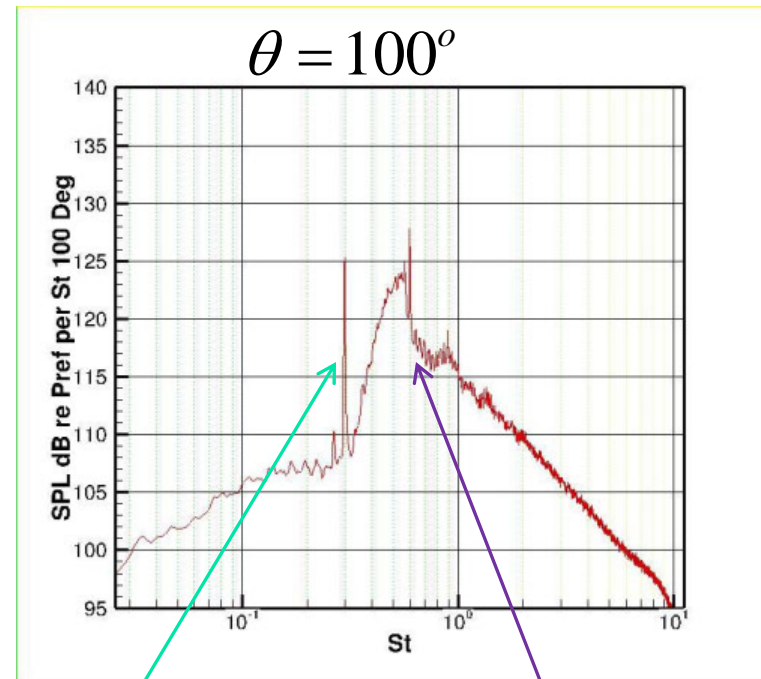


Supersonic Jet Noise

$$M_d = 1.0, M_j = 1.5, TTR=1.0$$



"Mixing noise"

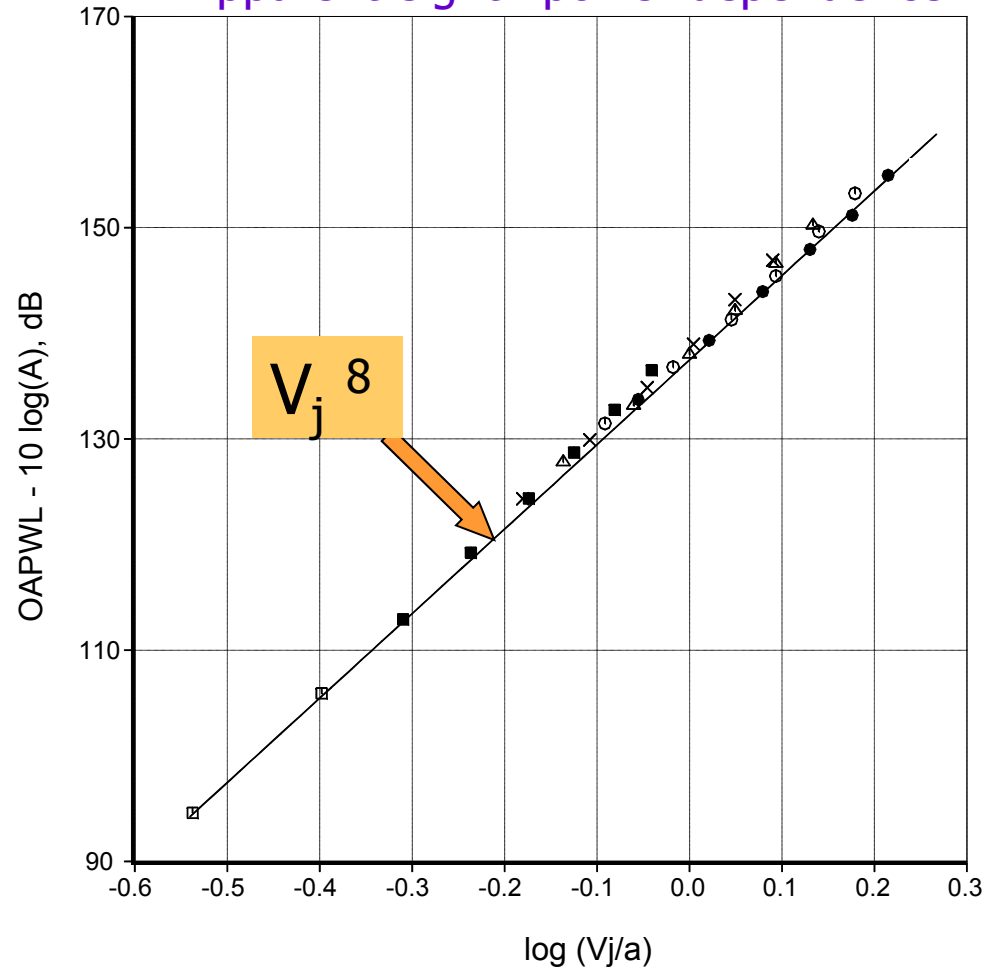


Screech

Broadband Shock-Associated Noise (BBSAN)

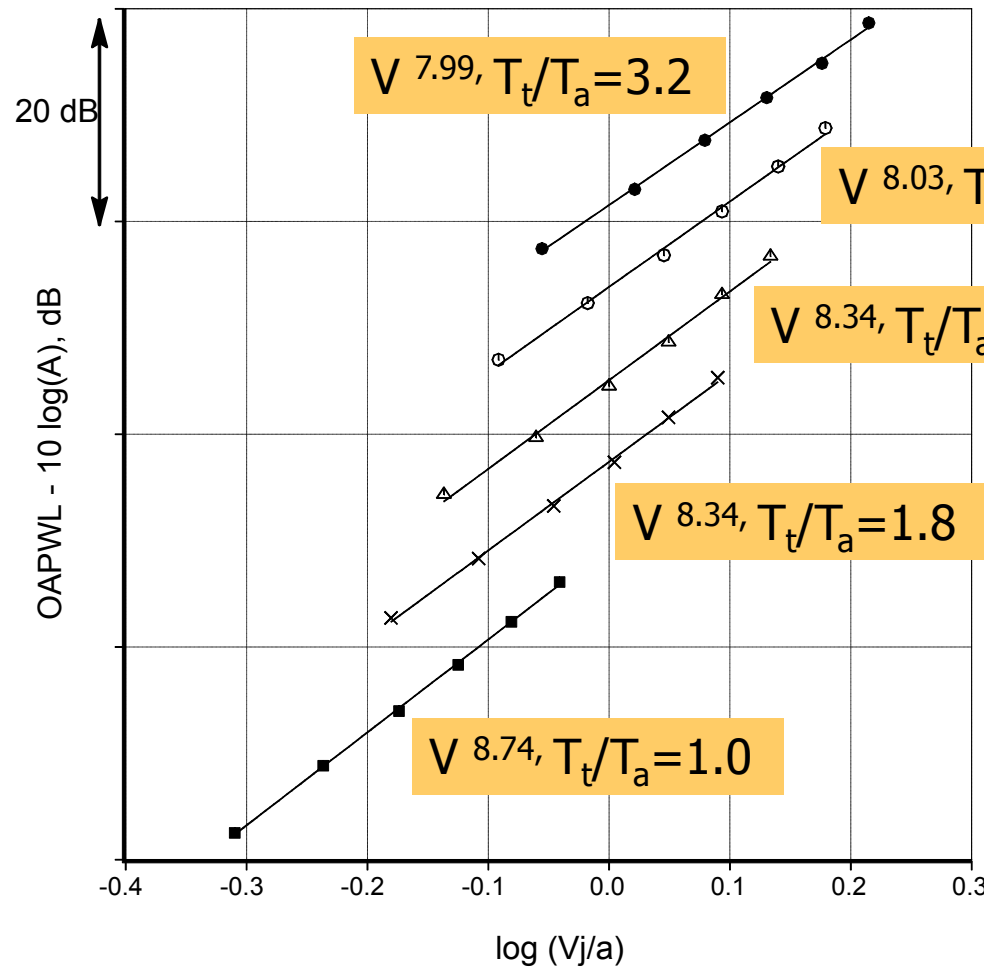
Velocity Dependence of Sound Power (OAPWL)

➤ Apparent eighth power dependence



Viswanathan (2004) JFM

Velocity Dependence of Sound Power (OAPWL)



$$n = n \left(\frac{T_t}{T_a} \right)$$

Excellent collapse of OAPWL with temperature ratio!

➤ no sixth power dependence even for $T_t/T_a=3.2!!$

Viswanathan (2004) JFM

Scaling Laws

- Viswanathan (2004, 2006)

$$\text{Sound power} \propto \left(\frac{V_j}{a} \right)^n, \quad n = n \left(\frac{T_t}{T_a} \right)$$

- Mixing noise spectra valid for all angles :

$$SPL(\theta, St) = F \left(\theta, St, \frac{T_t \text{ or } T_j}{T_a} \right) \left[\frac{V_j}{a} \right]^n, \quad n = n \left(\theta, \frac{T_t \text{ or } T_j}{T_a} \right)$$

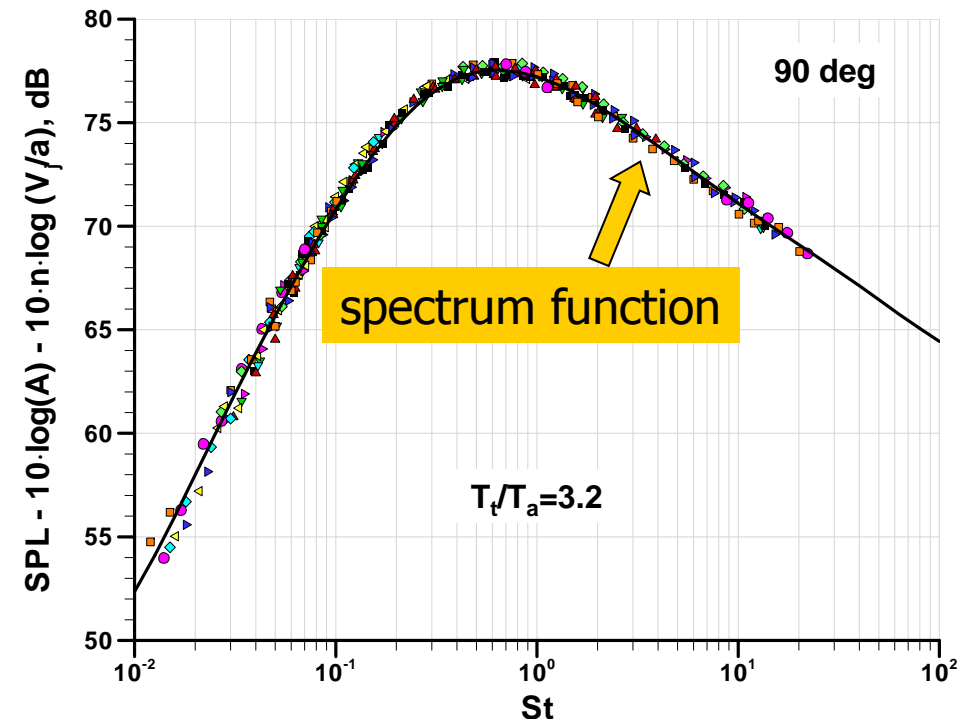
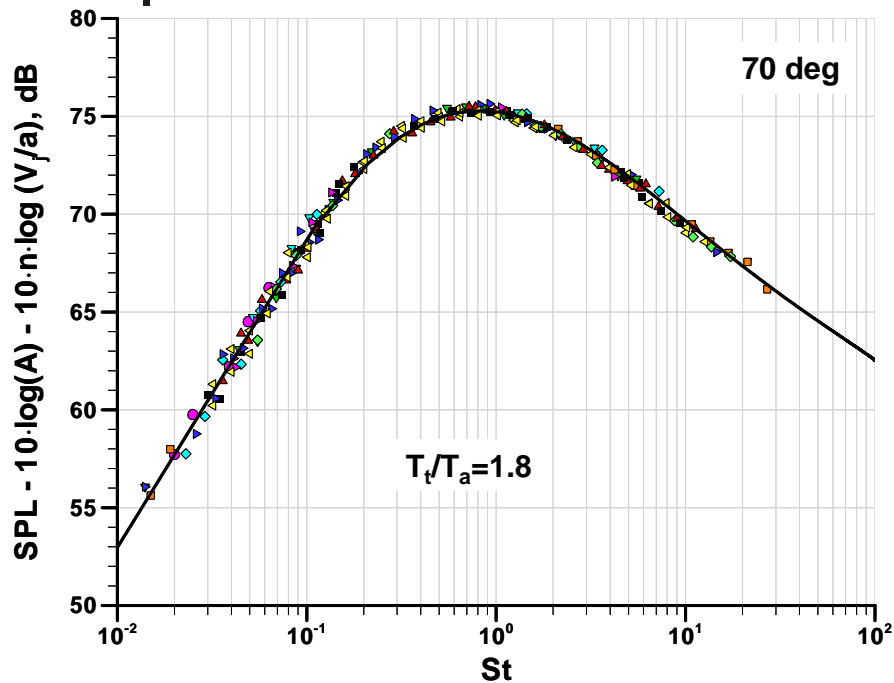
spectrum function

velocity exponent

- Explicitly identifies T_t/T_a or T_j/T_a as independent parameter
- Spectra defined by 3 parameters: θ , V_j/a , $T_{t \text{ or } j}/T_a$

Sample Normalized Spectra: PENN STATE

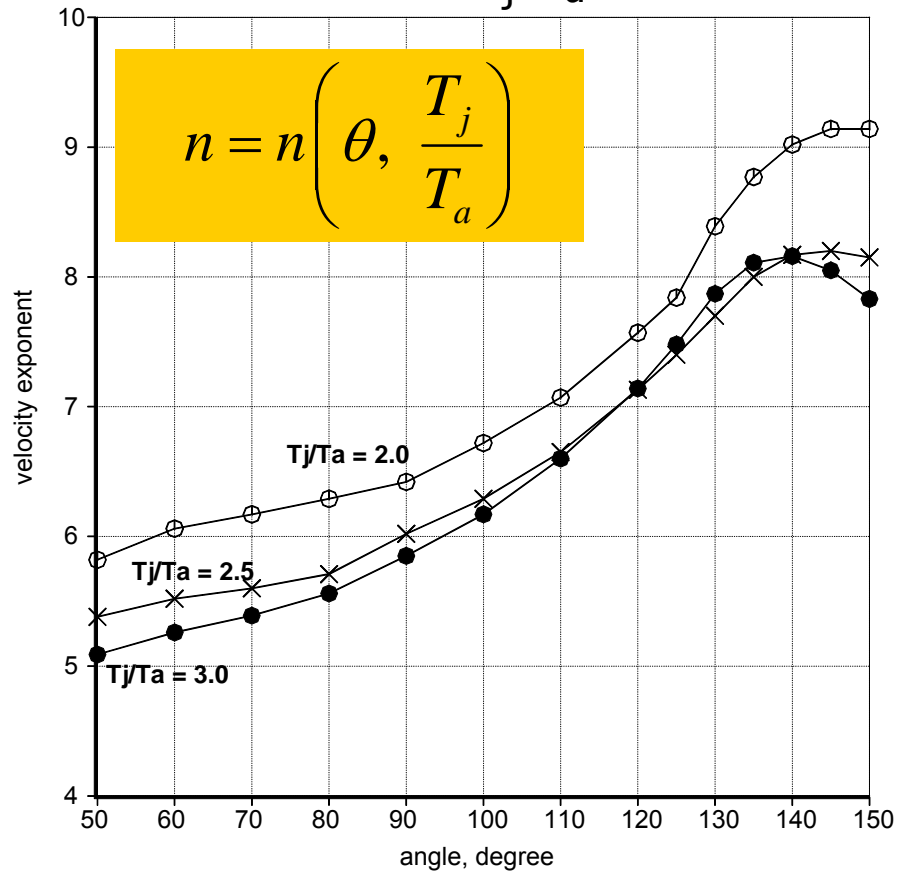
Fixed T_t/T_a



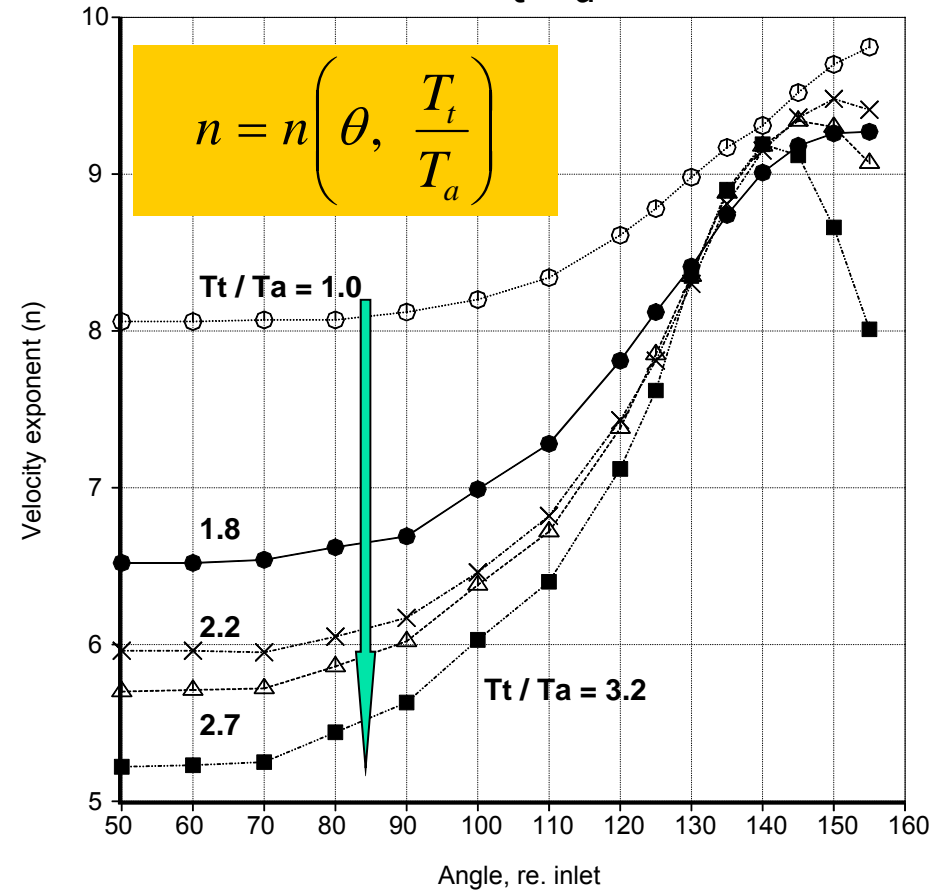
- Excellent collapse of spectra with correct exponent
- Perfect collapse over entire frequency (St) range
 - use of proper independent parameters critical

Variation of n with Angle and Temperature Ratio

fixed T_j/T_a



fixed T_t/T_a

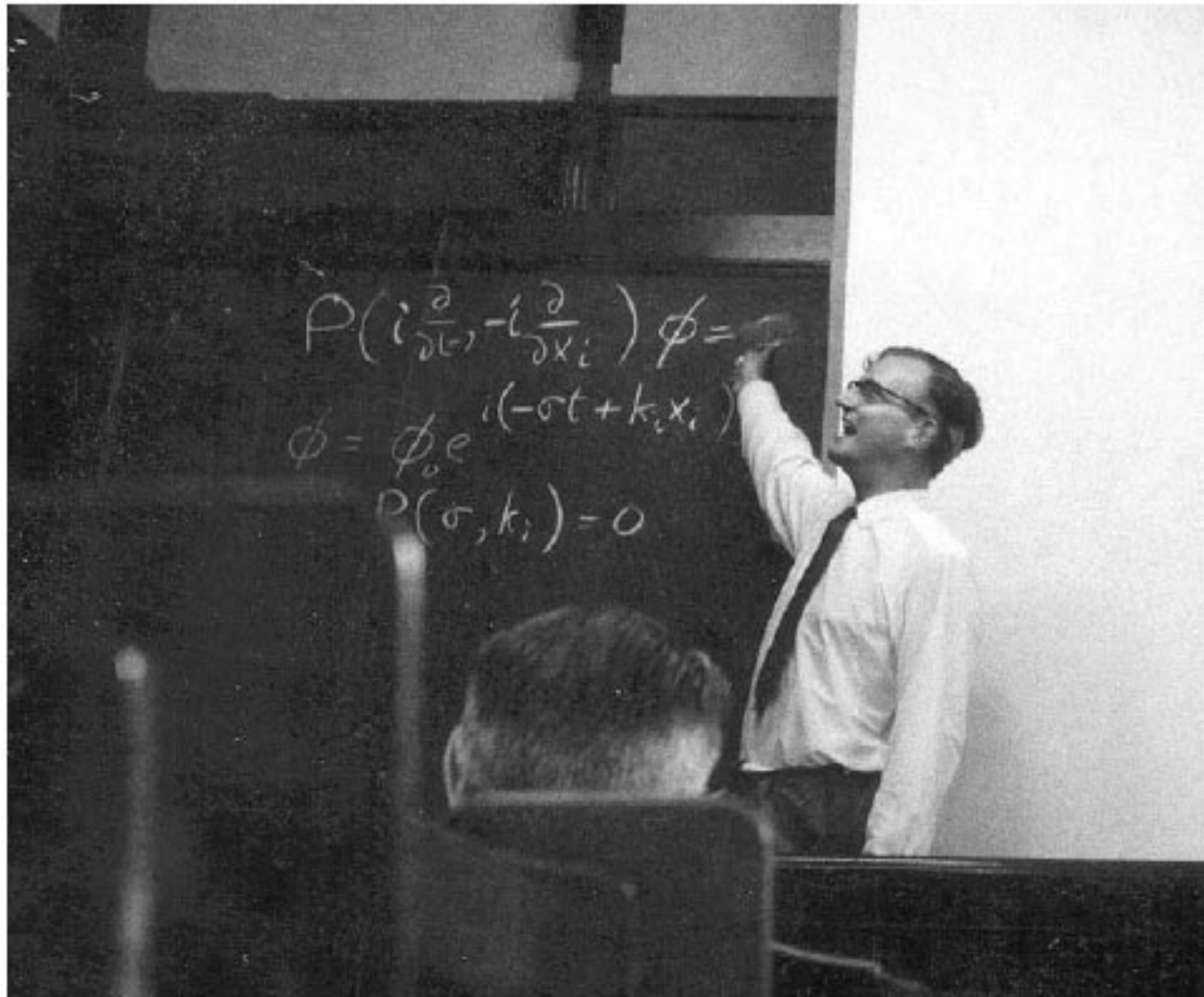


➤ similar trends for both temperature ratios

Theory and Predictions

- Lighthill's Acoustic Analogy
- Scaling Laws
- Mean Flow/Acoustic Interaction Effects
- Recent Acoustic Analogies
 - Mixing noise
 - Broadband Shock-Associated Noise
- Noise from Large Scale Structures
 - Wavepacket models
- Computational Approaches

Sir James Lighthill (1924-98)



Courtesy: Malcolm Crocker, "SIR JAMES LIGHTHILL AND HIS CONTRIBUTIONS TO SCIENCE"

Lighthill's Acoustic Analogy

- M. J. Lighthill, "On Sound Generated Aerodynamically. Part I: General Theory. Part II: Turbulence as a Source of Sound," *Proc. Roy. Soc. Lond.*, **A211** (1952) pp. 564-587. *Proc. Roy. Soc. Lond.*, **A222** (1954) pp. 1-32.

$$\frac{\partial \rho}{\partial t} + \frac{\partial}{\partial x_i} (\rho u_i) = Q(\mathbf{x}, t) \quad \times \frac{\partial}{\partial t}$$

Neglect viscous terms

and

$$\frac{\partial \rho u_i}{\partial t} + \frac{\partial \rho u_i u_j}{\partial x_j} = -\frac{\partial p}{\partial x_i} + f_i(\mathbf{x}, t) \quad \times \frac{\partial}{\partial x_i}$$

Lighthill's Acoustic Analogy

$$\frac{\partial^2 \rho}{\partial t^2} = \frac{\partial Q}{\partial t} - \frac{\partial f_i}{\partial x_i} + \frac{\partial^2 (\rho u_i u_j)}{\partial x_i \partial x_j} + \frac{\partial^2 p}{\partial x_i \partial x_i}$$

Subtract $c_o^2 (\partial^2 \rho' / \partial x_i \partial x_i)$ from **both** sides of the equation

$$\frac{\partial^2 \rho'}{\partial t^2} - c_o^2 \frac{\partial^2 \rho'}{\partial x_i \partial x_i} = \frac{\partial Q}{\partial t} - \frac{\partial f_i}{\partial x_i} + \underbrace{\frac{\partial^2 \rho u_i u_j}{\partial x_i \partial x_j} + \frac{\partial^2 p'}{\partial x_i \partial x_i} - c_o^2 \frac{\partial^2 \rho'}{\partial x_i \partial x_i}}_{\frac{\partial^2}{\partial x_i \partial x_j} [\rho u_i u_j + (p' - c_o^2 \rho') \delta_{ij}]}$$

Let

$$T_{ij} = \rho u_i u_j + (p - c_o^2 \rho) \delta_{ij} \quad \text{Lighthill stress tensor}$$

So that

$$\frac{\partial^2 \rho'}{\partial t^2} - c_o^2 \frac{\partial^2 \rho'}{\partial x_i \partial x_i} = \frac{\partial Q}{\partial t} - \frac{\partial f_i}{\partial x_i} + \frac{\partial^2 T_{ij}}{\partial x_i \partial x_j}$$

General Solution

In the absence of mass addition and forces

$$\square^2 \rho' = \frac{\partial^2 T_{ij}}{\partial x_i \partial x_j}$$

So the general solution in the far field is,

$$\rho'(\mathbf{x}, t) = \frac{1}{4\pi c_o x} \iiint_{V(\mathbf{y})} \int_{\tau} \frac{\partial^2 T_{ij}}{\partial y_i \partial y_j}(\mathbf{y}, \tau) \delta[|\mathbf{x} - \mathbf{y}| - c_o(t - \tau)] d\tau d\mathbf{y}$$

Finally,

$$\rho'(\mathbf{x}, t) = \frac{1}{4\pi c_o^4 x} \beta_i \beta_j \iiint_{V(\mathbf{y})} \frac{\partial^2 T_{ij}}{\partial t^2} \left(\mathbf{y}, t - \frac{x}{c_o} \right) d\mathbf{y} \quad \rho' \sim c_o^{-4} x^{-1} (\rho_o u^2) \left(\frac{u^2}{\ell^2} \right) \ell^3$$

Noise Scaling

$$\rho'(\mathbf{x}, t) \sim c_o^{-4} x^{-1} \left(\rho_o u^2 \frac{u^2}{\ell^2} \right) \ell^3 \sim \rho_o \left(\frac{\ell}{x} \right) m^4 \quad I = \overline{p'u'} = \frac{\overline{p'^2}}{\rho_o c_o} = \frac{\overline{\rho'^2} c_o^4}{\rho_o c_o}$$

with directionality given by $\beta_i \beta_j$. Now, the intensity

$$I = \frac{c_o^3}{\rho_o} \overline{\rho'^2} \sim \frac{c_o^3}{\rho_o} \rho_o^2 \left(\frac{\ell}{x} \right)^2 m^8 \sim \rho_o \left(\frac{\ell}{x} \right)^2 u^3 m^5$$

Thus,

$$\text{Total energy flux (power)} \sim \rho_o \ell^2 u^3 m^5$$

Power = rate of change
of energy

$$\text{Power of source} \sim \left(\rho_o u^2 \ell^3 \right) \left(\frac{u}{\ell} \right) \sim \rho_o u^3 \ell^2$$

So that

$$\text{Acoustic efficiency; } \eta = \frac{\text{Acoustic power}}{\text{Source power}} \sim m^5 \ll 1$$

Jet Noise Scaling

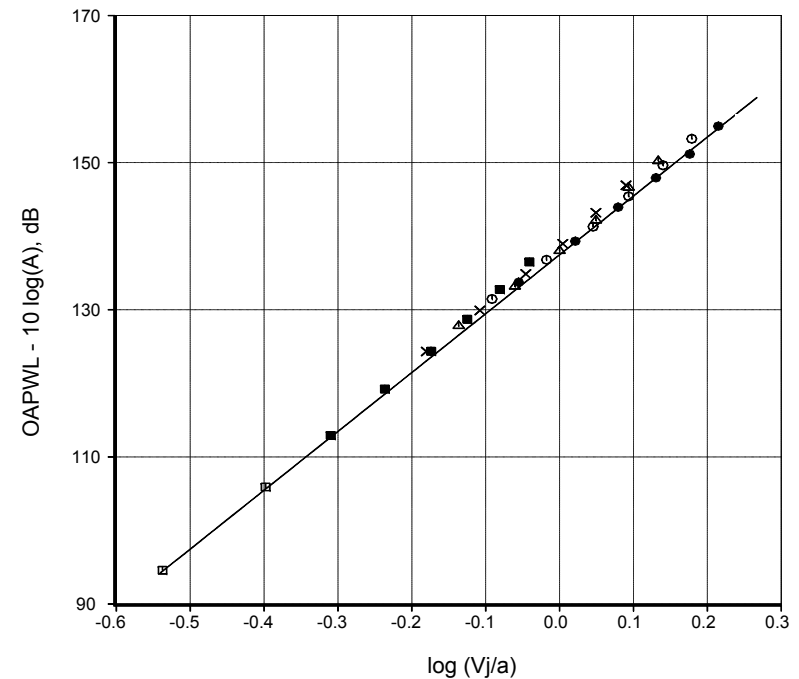
Assume that $\ell \sim d_j$ and $u \sim U_j$

Recall that $P_a \sim \rho_o u^3 \ell^2 m^5$

Acoustic Power: $P_a \sim \rho_o U_j^3 d_j^2 M_j^5$

$$P_a \sim \frac{\rho_o}{c_o^5} d_j^2 U_j^8$$

This is Lighthill's "Eighth Power Law"

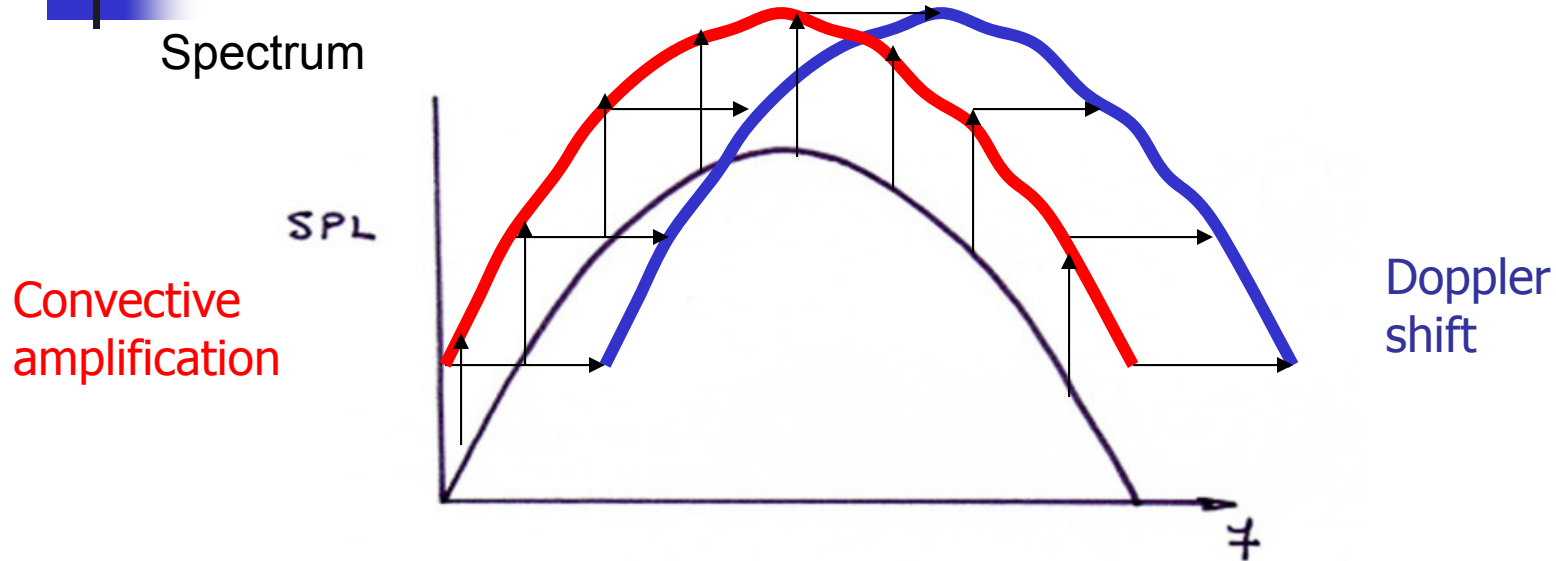


Effects of Source Convection

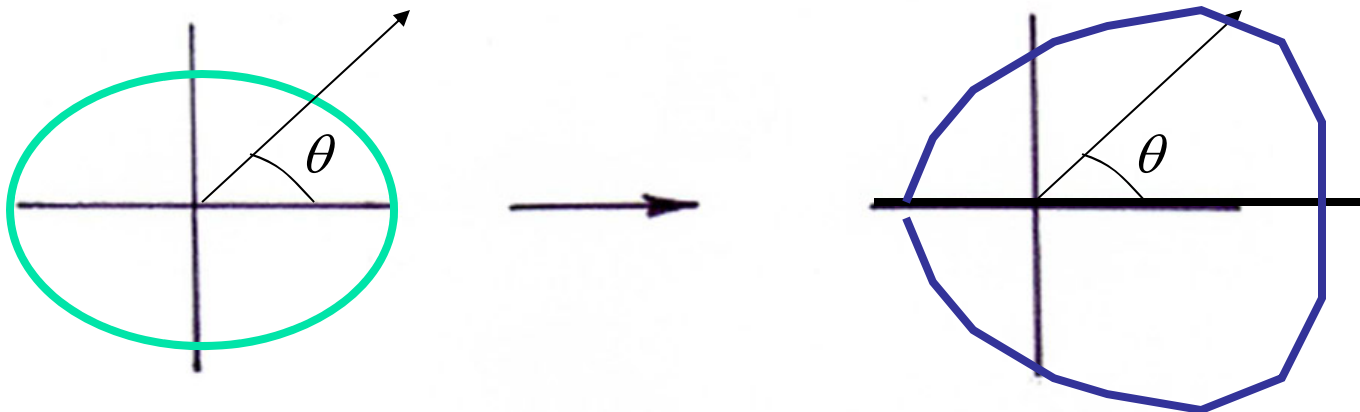
- Doppler shift in frequency
- “Convective Amplification”
 - Apparent change in frequency
 - Effective increase in source length (in direction of observer)
 - Offset by finite length of source region
- Gives five powers of Doppler factor

$$I \sim \rho_o c_o^3 \left(\frac{\ell}{x} \right)^2 \frac{m^8}{\left[(1 - M_c \cos \theta)^2 + m^2 \right]^{5/2}}$$

Summary of Convection Effects



Directivity



Jet Noise Spectra

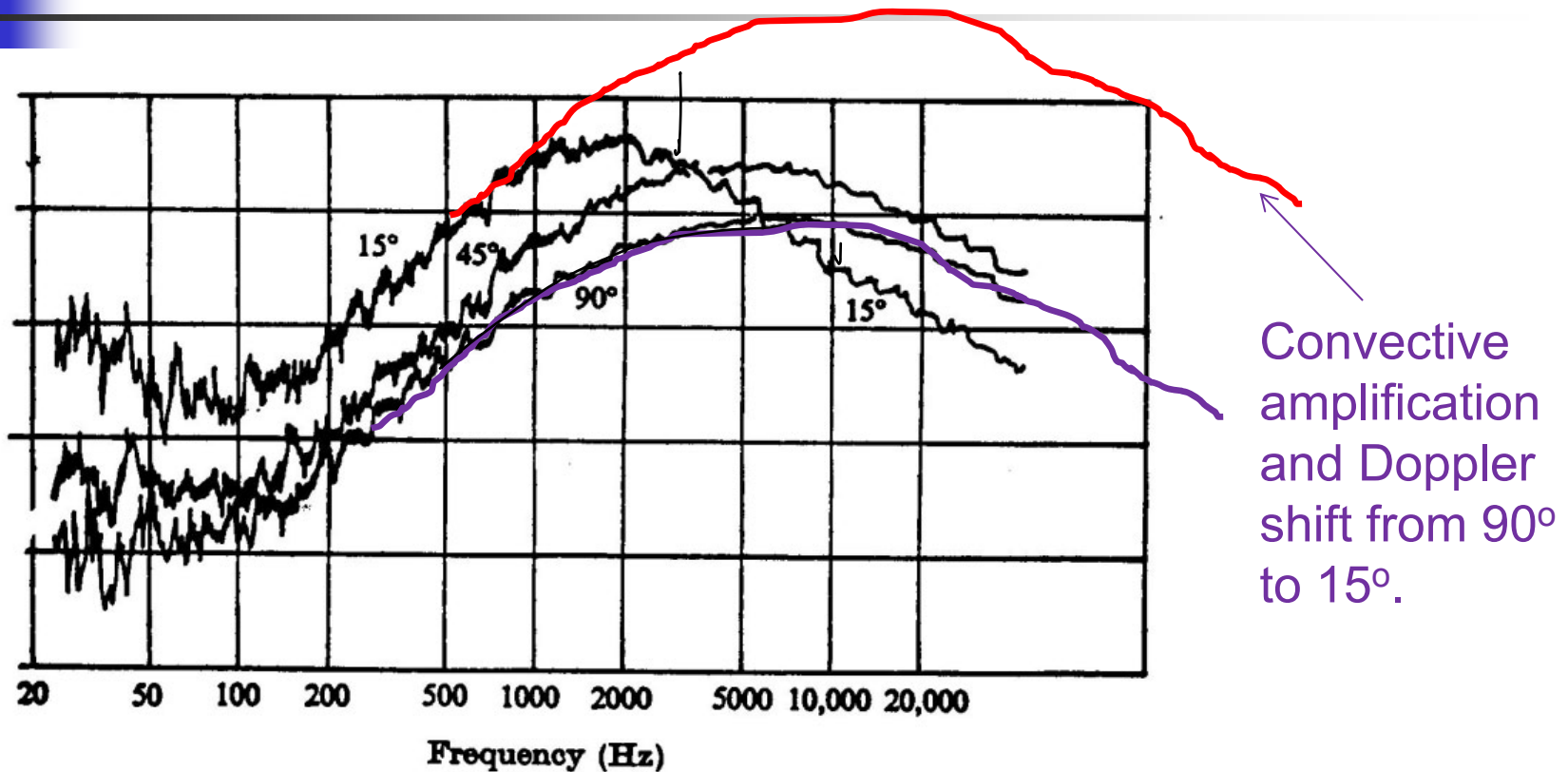


FIGURE 6. $\frac{1}{3}$ -octave spectra at 15°, 45° and 90° for jet velocity of 195 m/s.

Lush (1971)

Mean Flow/Acoustic Interactions

- Analysis developed by G. M. Lilley (1974)
- Details given by R. Mani (1976)
- Fundamental idea is to only retain terms on the left hand side of an acoustic analogy (the propagator) that are linear in the fluctuations. The right hand side (the equivalent sources) are at least second order in the fluctuations about the mean flow.
- Compressible equations of motion formulated in terms of *the logarithm of the thermodynamic properties*
- Originally used by Lord Rayleigh
 - "Theory of Sound," Vol. II: 352



Mean Flow Effects: Lilley's Equation

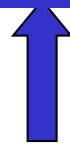
Lilley (1972) noted that for a parallel mean flow, $\bar{u}_i = U(x_2) \delta_{i1}$

The RHS reduces to,

$$\frac{\partial u_j}{\partial x_i} \frac{\partial u_k}{\partial x_j} \frac{\partial u_i}{\partial x_k} = 3 \frac{dU}{dx_2} \frac{\partial u'_k}{\partial x_1} \frac{\partial u'_2}{\partial x_k} + \frac{\partial u'_j}{\partial x_i} \frac{\partial u'_k}{\partial x_j} \frac{\partial u'_i}{\partial x_k}$$

This is quadratic in the fluctuations.

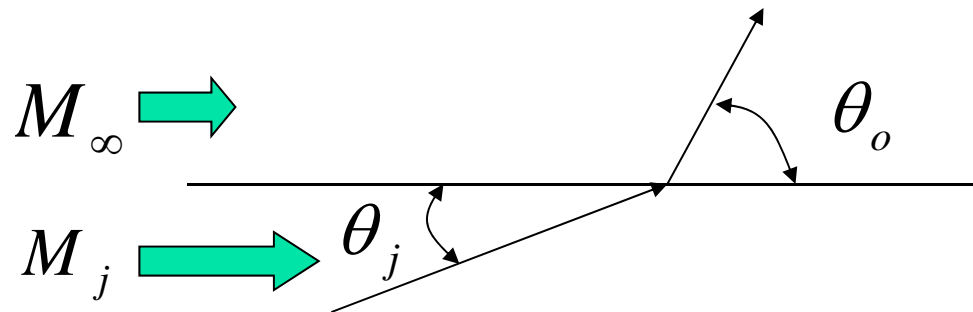
$$\frac{1}{c_o^2} \frac{\bar{D}^3 p'}{Dt^3} + 2 \frac{dU}{dx_2} \frac{\partial^2 p'}{\partial x_i \partial x_2} - \frac{\bar{D}}{Dt} \left\{ \frac{\partial^2 p'}{\partial x_i \partial x_i} \right\} = -2\rho_o \left\{ 3 \frac{dU}{dx_2} \frac{\partial u'_k}{\partial x_1} \frac{\partial u'_2}{\partial x_k} + \frac{\partial u'_j}{\partial x_i} \frac{\partial u'_k}{\partial x_j} \frac{\partial u'_i}{\partial x_k} \right\} + L(x_i, t)$$



Lilley's Equation

Physical Interpretation

Simple problem with uniform temperatures



Axial wavelength inside the jet,

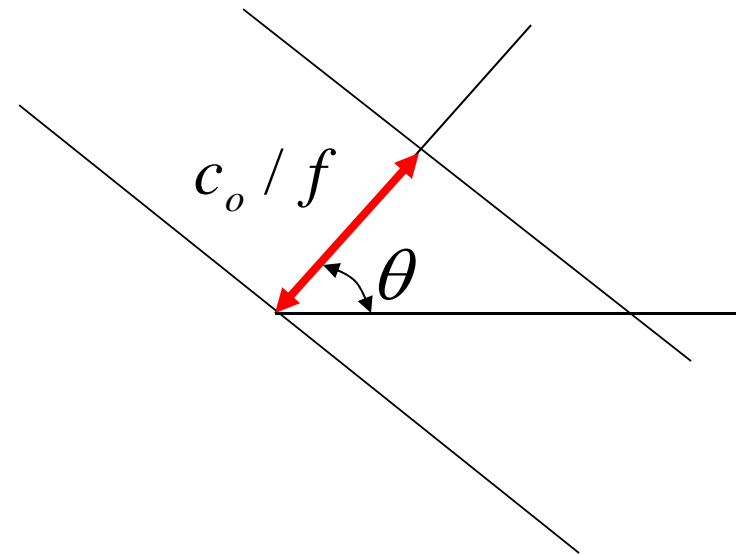
$$\lambda_x = \frac{c_o}{f} \left\{ \frac{1}{\cos \theta_j} + M_j \right\}$$

Axial wavelength outside the jet,

$$\lambda_x = \frac{c}{f} \left\{ \frac{1}{\cos \theta_\infty} + M_\infty \right\}$$

These must be equal at the interface, so

$$\frac{1}{\cos \theta_j} + M_j = \frac{1}{\cos \theta_\infty} + M_\infty$$



Physical Interpretation

$$\theta_{\infty} = \cos^{-1} \left\{ \frac{1}{M_j - M_{\infty} + 1/\cos \theta_j} \right\}$$

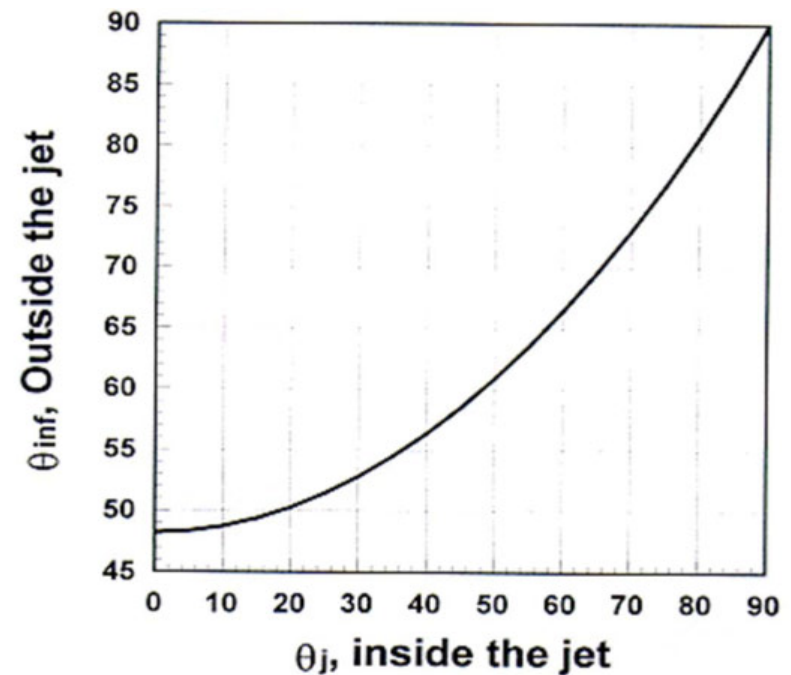
Now, $\cos \theta_j \leq 1$, so the smallest value of θ_{∞} occurs when $\theta_j = 0$. This gives the critical value of the radiation angle : the edge of the zone of silence

$$\theta_{crit} = \cos^{-1} \left\{ \frac{1}{M_j - M_{\infty} + 1} \right\}$$

$$M_j = 0.5,$$

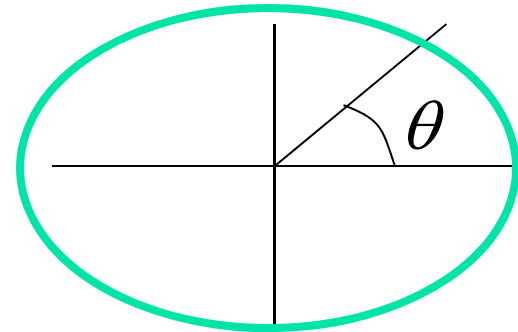
$$M_o = 0.0$$

$$\theta_c = \cos^{-1}(2/3) = 48.2^{\circ}$$

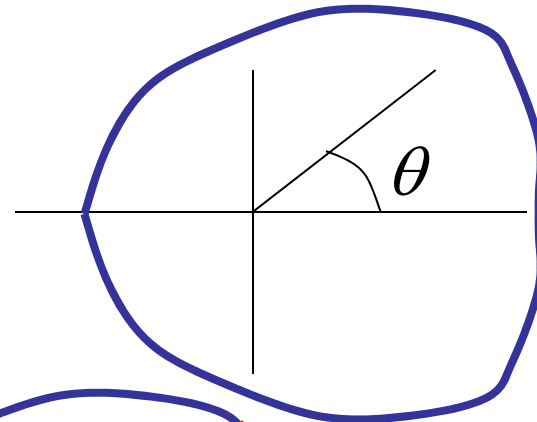


Overall Far Field Directivity

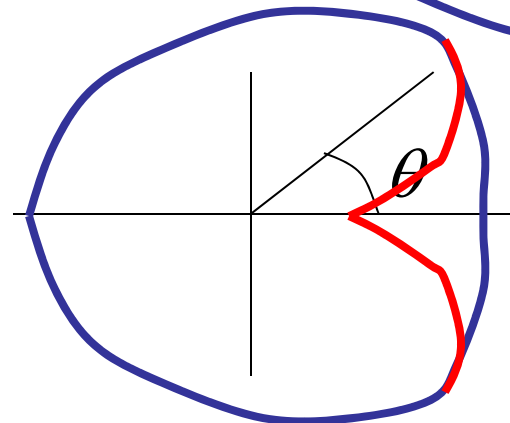
1) Source directivity



2) Convective amplification



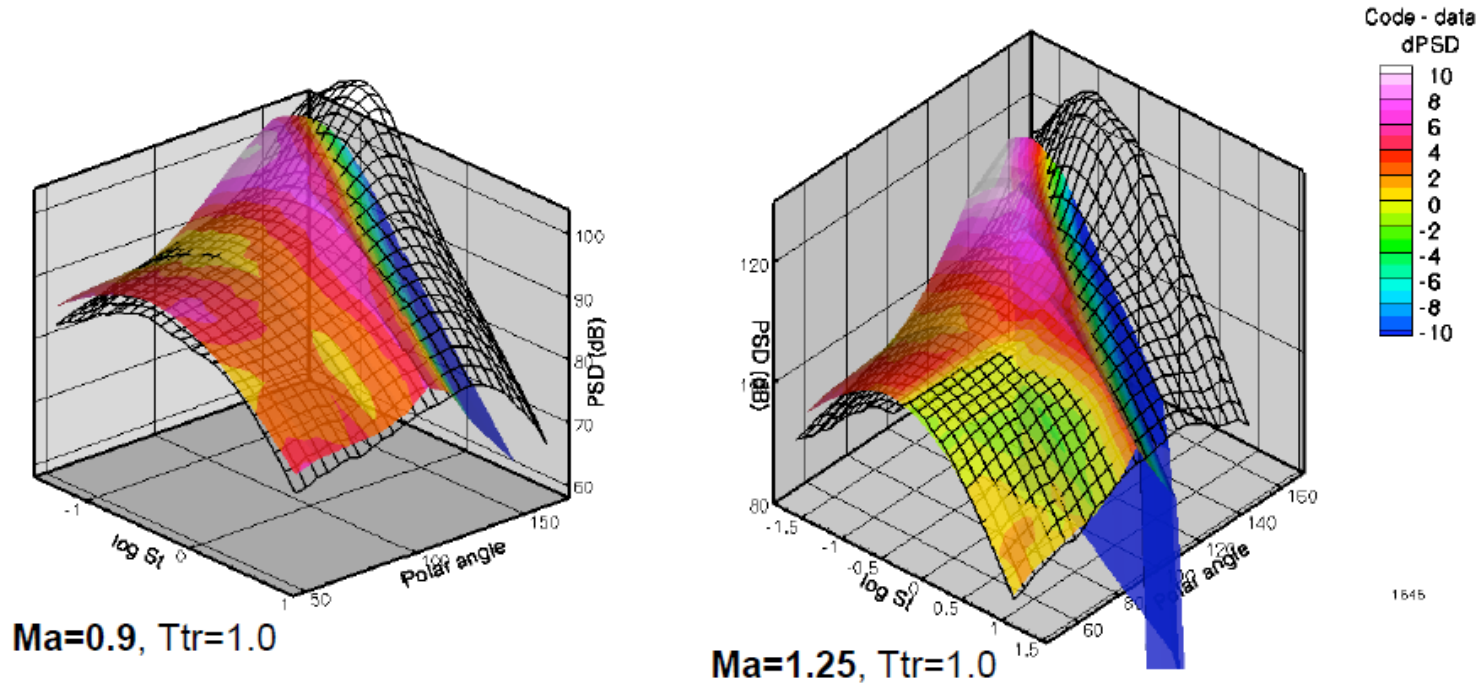
3) Mean flow/acoustic interactions



JeNo Predictions

Predictions based on Lilley's equation for propagation

Mani, Gliebe, Balsa, Khavaran (MBGK)



Bridges (2008)

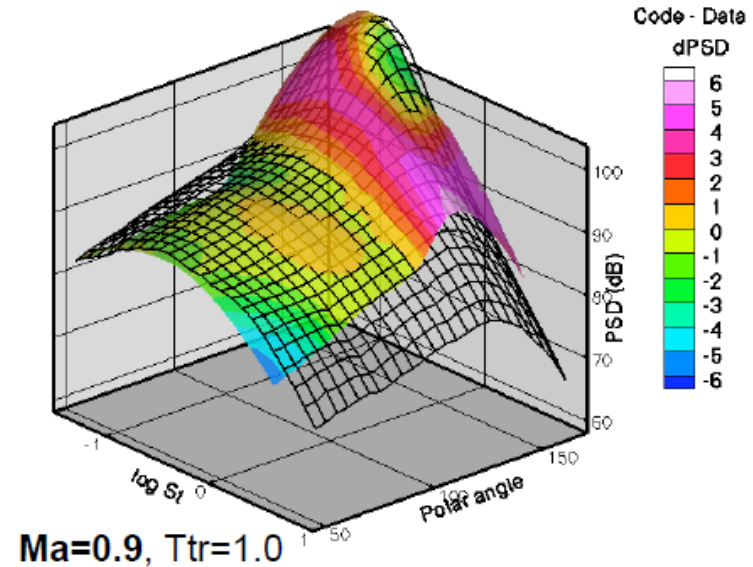
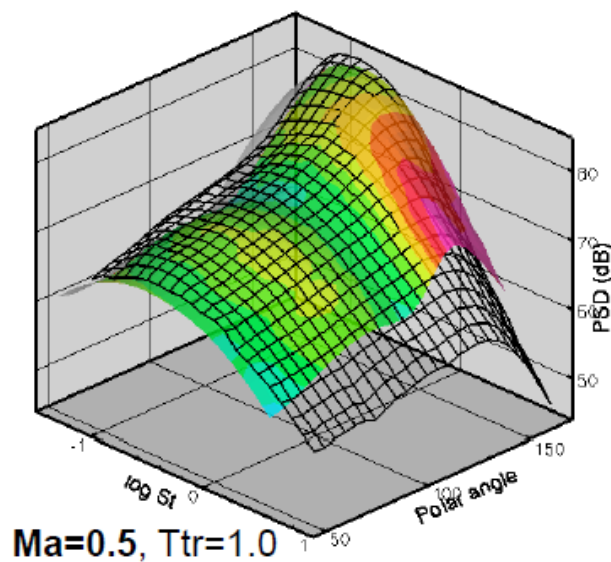


Goldstein & Leib (2008)

- Goldstein's acoustic analogy – linearized equations about Favre-averaged steady base flow
- Asymptotic solutions for propagation in the diverging jet flow
- Source statistics based on (limited) flow measurements
- Limited tests with convectively subsonic (though high speed) jets

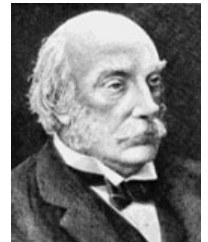
Goldstein & Leib (2008)

- Much better agreement with data at aft angles
 - Nonparallel flow assumption and advanced turbulent source model
- Has proper trend with increased speed



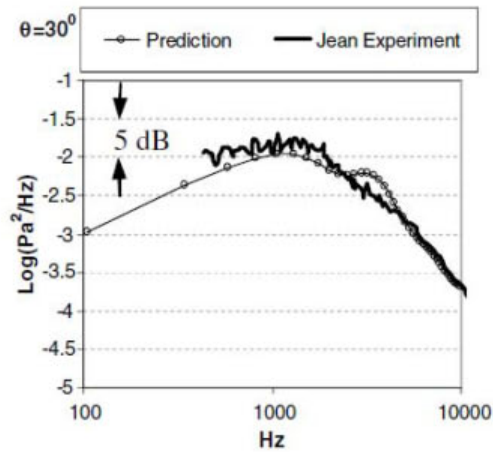
Karabasov et al. (2010)

- Also based on Goldstein's acoustic analogy
- Numerical solutions for propagation in the diverging jet flow
- Source statistics based on LES simulations
- Also limited so far to convectively subsonic jets

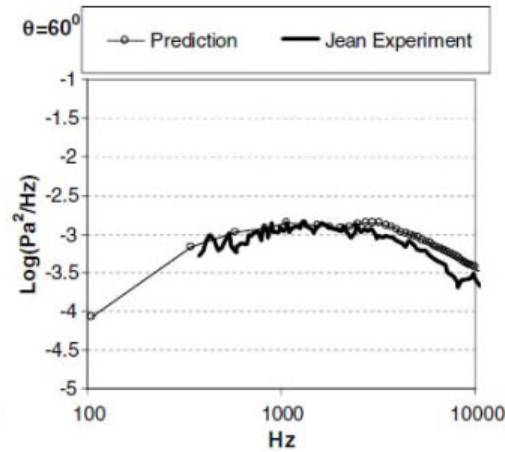


Karabasov et al. (2010)

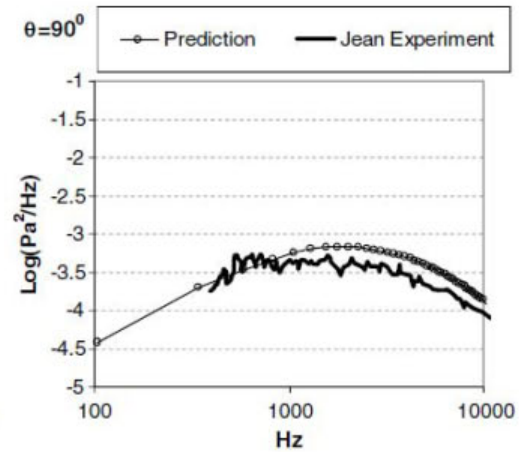
$$M_d = 1.0, \quad M_j = 0.75, \quad TTR = 1.0$$



a)



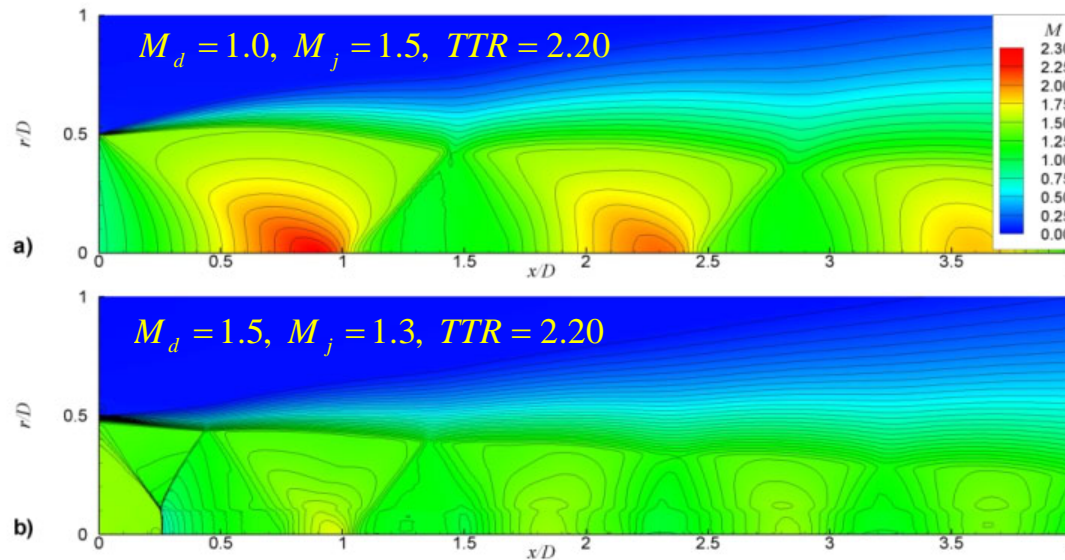
b)



c)

Broadband Shock-Associated Noise (BBSAN)

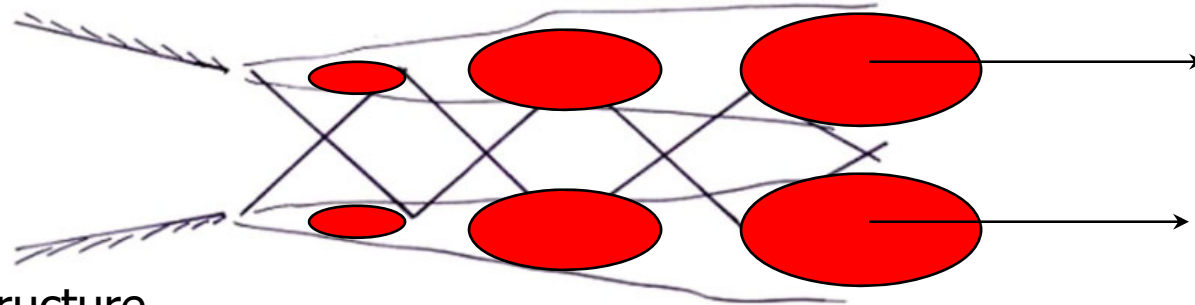
- Generated by the interaction of the turbulence in the jet shear layer with the jet's shock cell structure



Underexpanded

Overexpanded

Physical Model



Shock cell structure

$$p_s = \sum_{n=0}^{\infty} a_n e^{i k_n x} + \text{complex conjugate}$$

Instability waves

$$p_i = b_n e^{i(\alpha x - \omega t)} + \text{complex conjugate}$$

Weak interaction gives pattern

$$p_c \sim p_s \times p_i$$

$$p_c \sim a_n b_n \exp\{-i[(\alpha + k_n)x - \omega t]\} +$$

$$a_n b_n^* \exp\{-i[(\alpha - k_n)x - \omega t]\} + \mathbf{C.C.}$$

Efficient radiation (upstream)

BBSAN Models

- Harper-Bourne & Fisher (1973)
 - Interaction generates point sources that radiate constructively
- Tam (1987)
 - Shock cells modeled as standing wave (Prandtl) and large-scale turbulent structures modeled as instability waves
- Morris & Miller (2010)
 - Shock cells calculated from RANS solution and acoustic analogy used to describe noise radiation statistics.
 - Includes axisymmetric, dual stream and rectangular jet predictions

Present Approach

- Based on the Euler equations in terms of the logarithm of pressure and velocity (Rayleigh: 1877)
- Variables separated into four components
 - Long time average
 - Shock cell structure
 - Coherent turbulent fluctuations
 - Fluctuations associated with the interaction of the turbulent fluctuations with the shock cells – this is the Broadband Shock-Associated Noise (BBSAN)



Present Approach

- Equations are separated into a linear operator (the linearized Euler equations: LEE) and interaction terms (sources)
- Solution for the far field pressure written in terms of the vector Green's function for the LEE
 - Use reciprocity/adjoint principle (Rayleigh: 1877)
- Pressure autocorrelation and spectral density is obtained
- Model introduced for turbulence statistics
- Shock cell represented in terms of its wavenumber content
- Expression obtained for spectral density in terms of quantities provided by a RANS CFD solution with a two-equation turbulence model



Final Prediction Formula

Spectral density

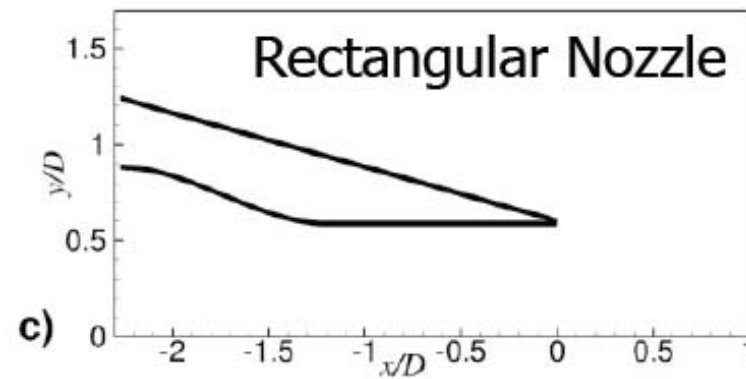
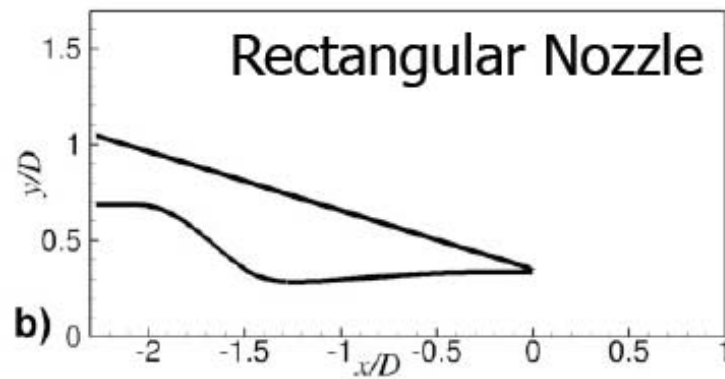
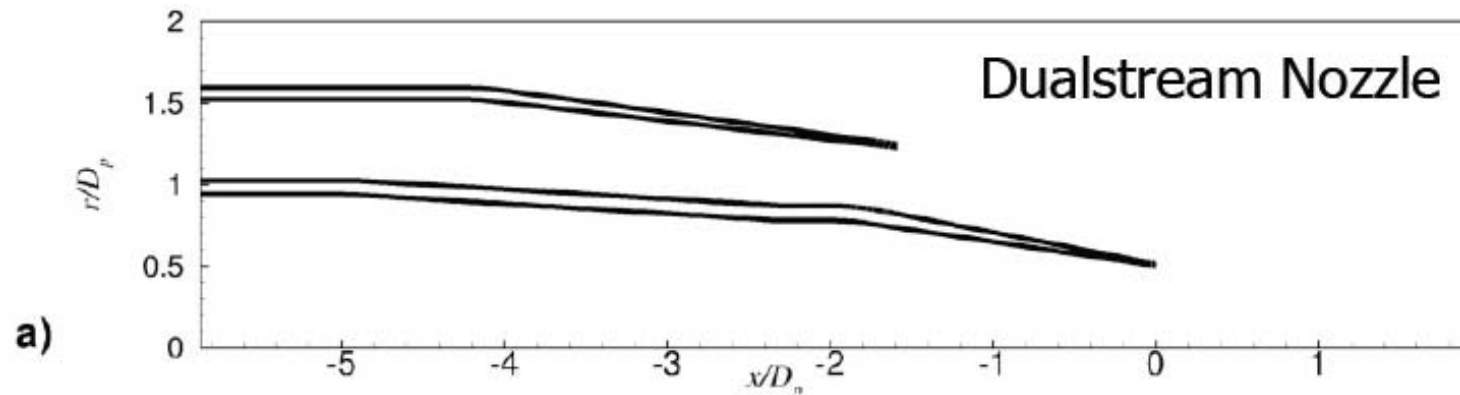
Adjoint Green's functions

$$\begin{aligned}
 S(\mathbf{x}, \omega) = & \sqrt{\pi} c_\infty^2 \int_{-\infty}^{\infty} \cdots \int_{-\infty}^{\infty} \left\{ \sum_{n=1}^{\infty} \sum_{m=1}^{\infty} \pi_g^{n*}(\mathbf{x}, \mathbf{y}, \omega) \pi_g^m(\mathbf{x}, \mathbf{y}, \omega) \right. \\
 & \times p_s(\mathbf{y}) \tilde{p}_s(k_1, y_2, y_3) \exp(-ik_1 y_1) \frac{a_{nm} K l_\perp^2 \tau_s}{l} \left. \right\} \\
 & \times \frac{\exp\left[-l^2 (\omega \cos \theta / a_\infty - k_1)^2 / 4 - \omega^2 l^2 \sin^2 \theta / (4a_\infty^2)\right]}{\left[1 + (1 - M_c \cos \theta + uk_1 / \omega)^2 \omega^2 \tau_s^2\right]} dk_1 d\mathbf{y}
 \end{aligned}$$

Shock cell structure

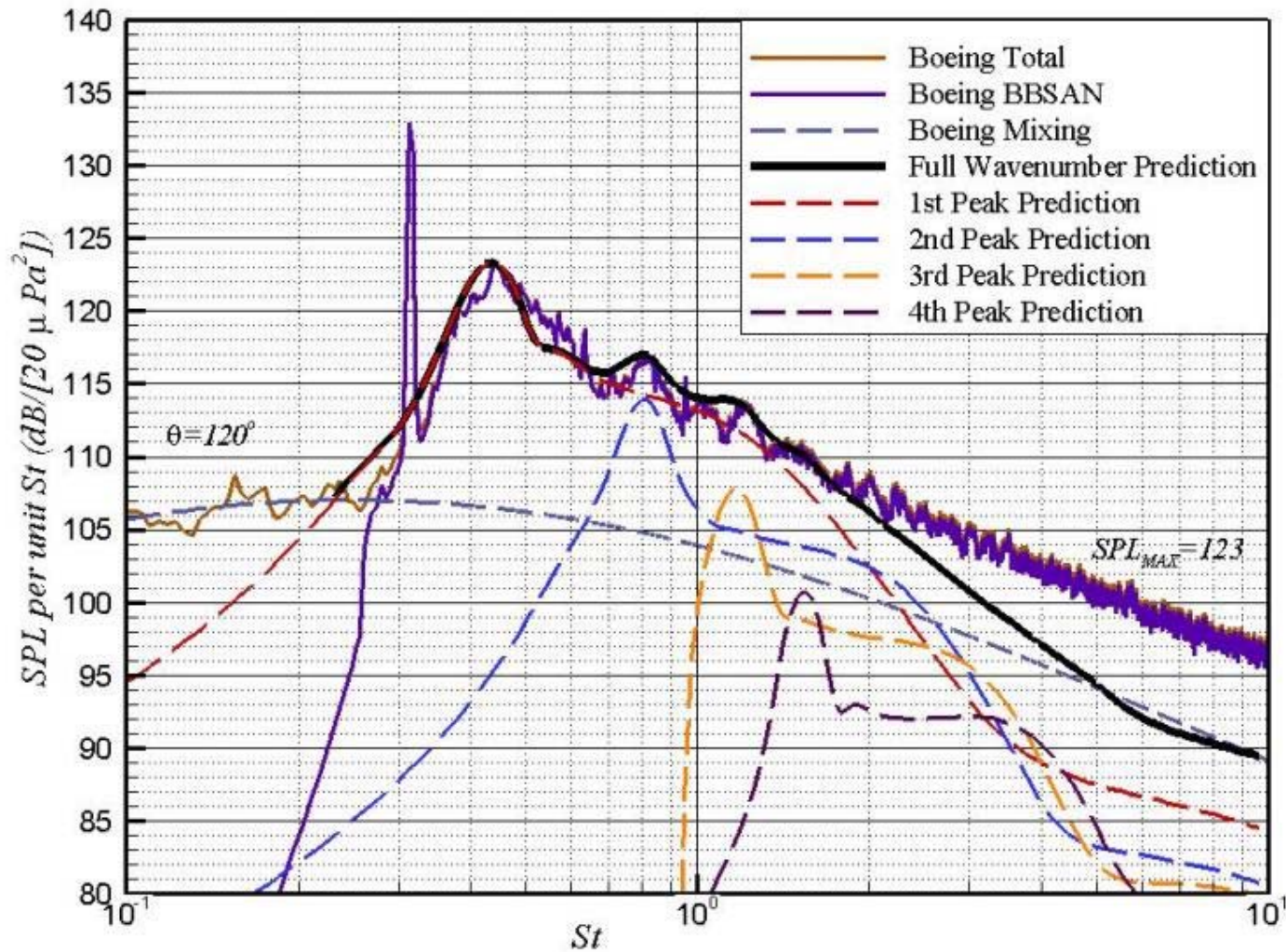


Nozzle Geometries



BBSAN Prediction

$$M_d = 1.0, M_j = 1.5, TTR = 1.0$$



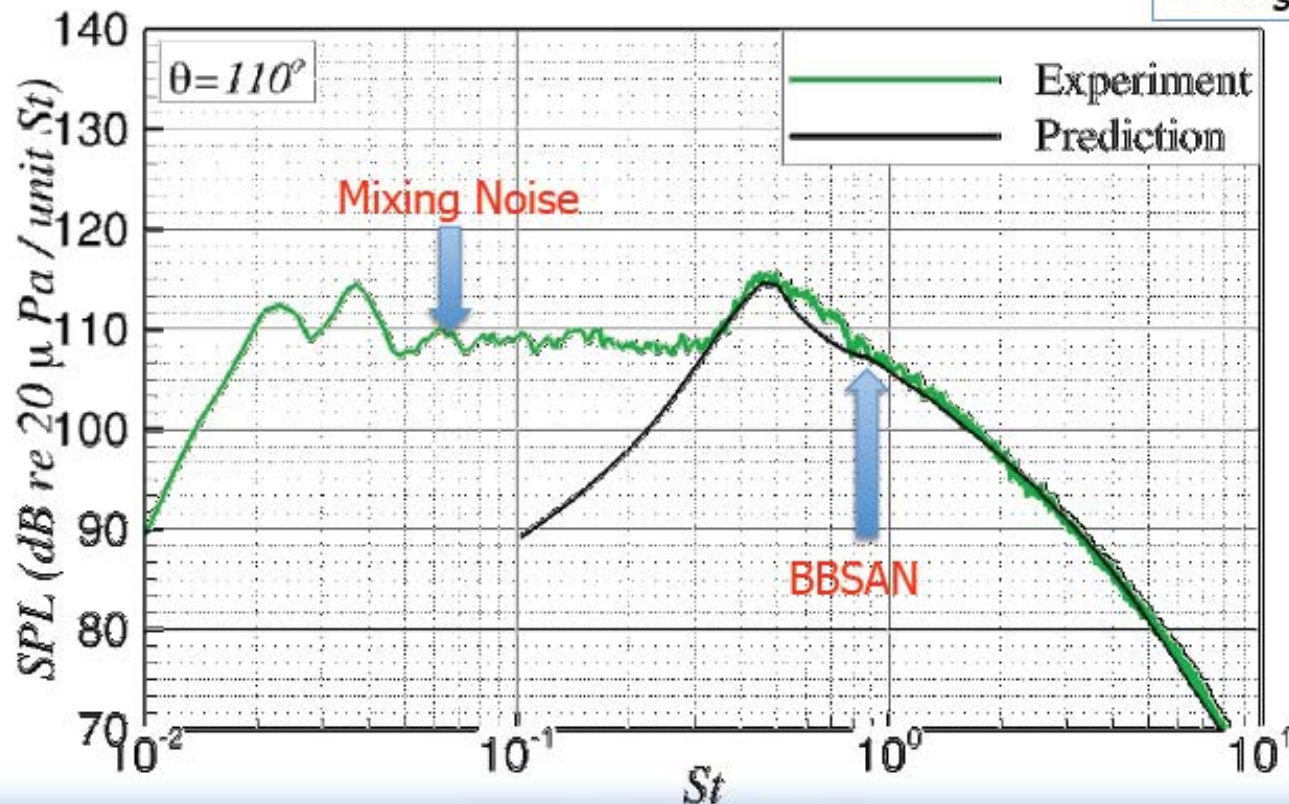


BBSAN Prediction Near Sideline

Prediction near sideline location

Little shear layer effects

$$\begin{aligned} M_{jp} &= 1.28 \\ M_{js} &= 0.84 \\ TTR_p &= 1.60 \\ TTR_s &= 1.00 \end{aligned}$$

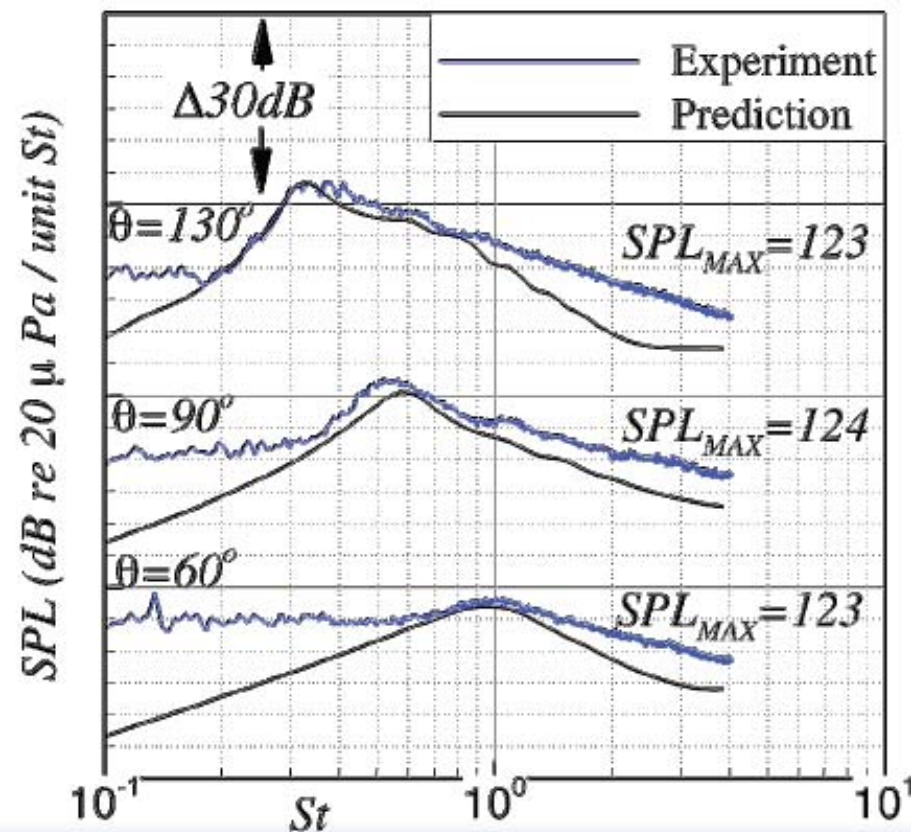




Rectangular Jet BBSAN Predictions

Predictions of Secondary BBSAN peaks

Other predictions similar



$$M_{jp} = 1.70$$
$$TTR_p = 1.00$$

Alternative View

- Turbulent jet mixing is controlled by large scale structures
- Individual frequency components grow and decay in the axial direction
- If the convection velocity of the structures is supersonic there is a direct link between the turbulence and the radiated noise
- Analysis and experiments have shown that the large scale structures can be described as **instability waves**



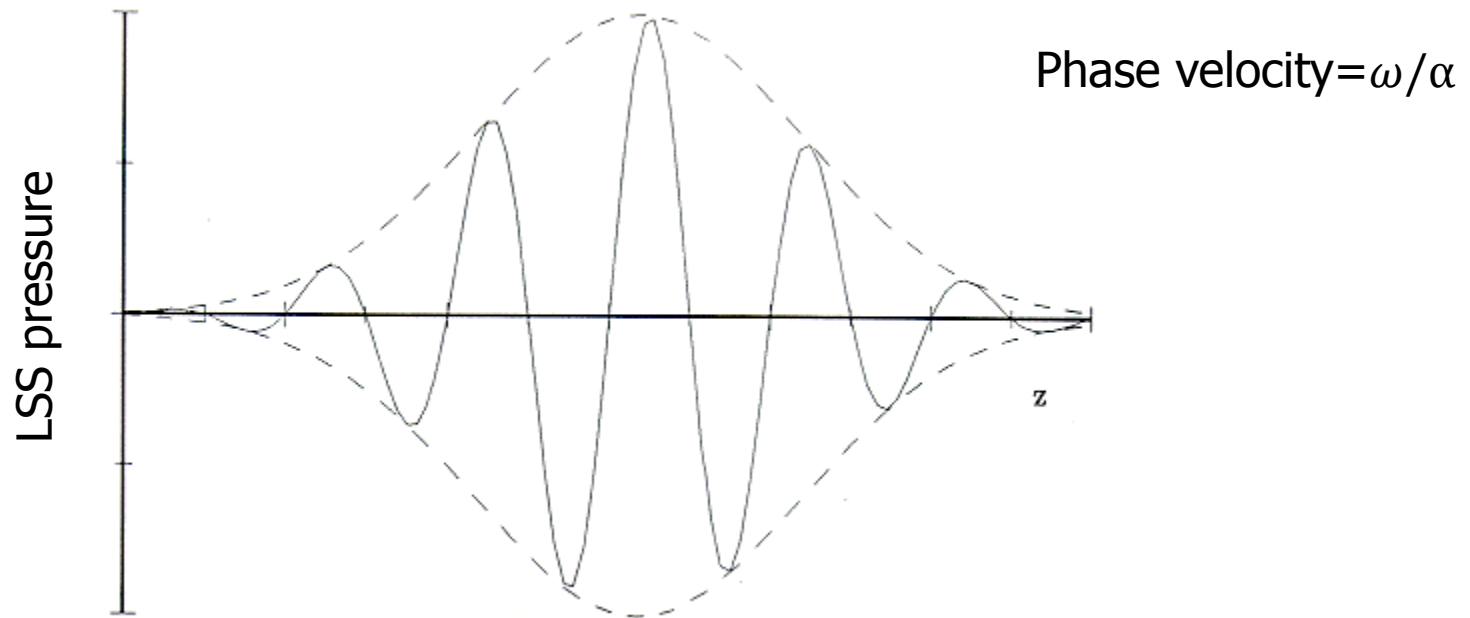
Brown & Roshko (1974)



o.
 $M_j = 0.76$
 $T_1 = 291 \text{ K}$
 $St_j = 0.28$
 $L_e = 143 \text{ dB}$

Lepicovsky et al. (1986)

Wavepacket Model



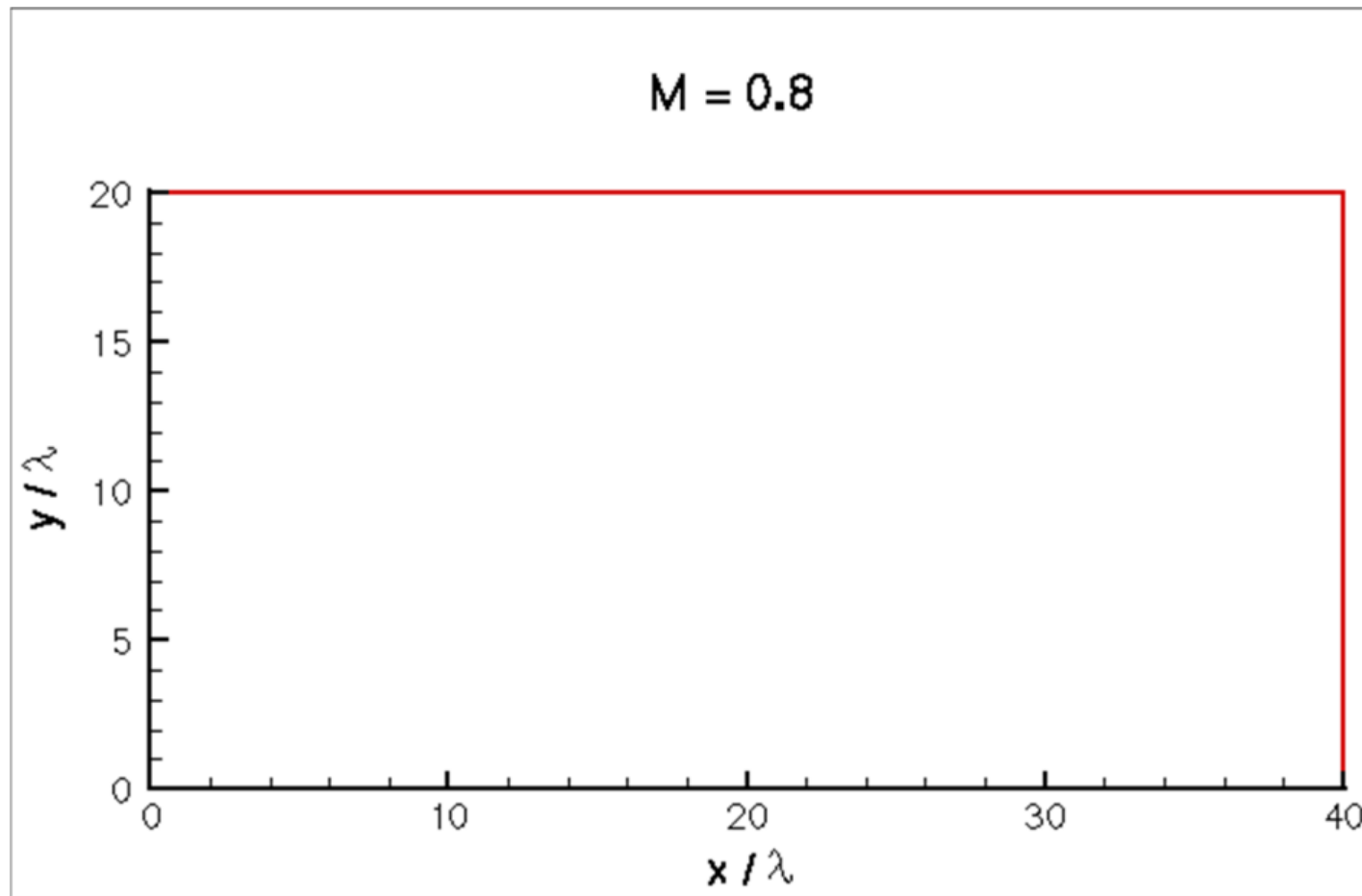
$$p(z,t) = \Re \left\{ A(z) \exp \left[i(\alpha z - \omega t) \right] \right\}$$

Amplitude envelope

Traveling wave

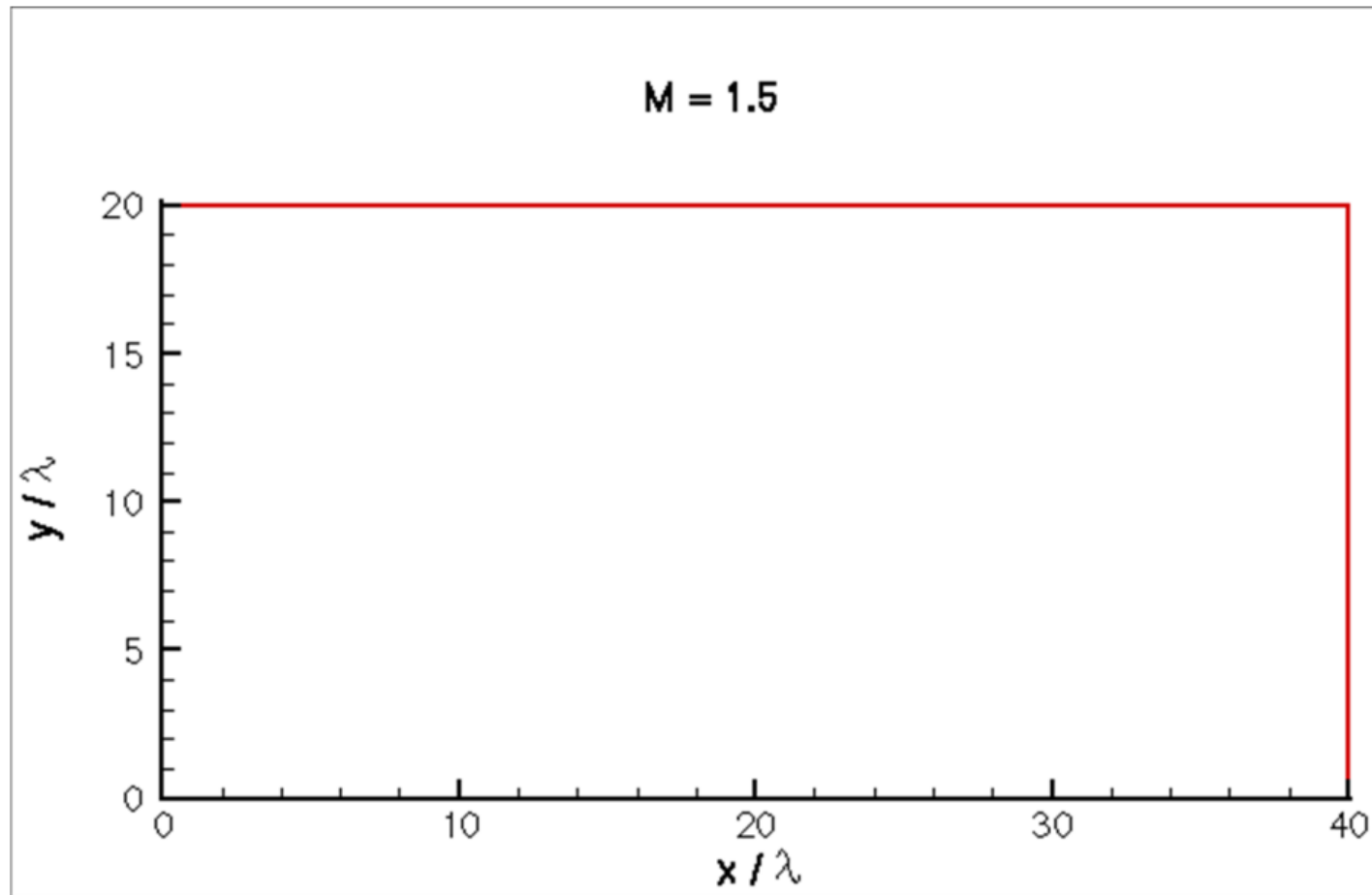
Noise From Large Scale Structures (Wavepackets)

Wavy Wall Analogy: Subsonic Phase Velocity



Noise From Large Scale Structures (Wavepackets)

Wavy Wall Analogy: Supersonic Phase Velocity

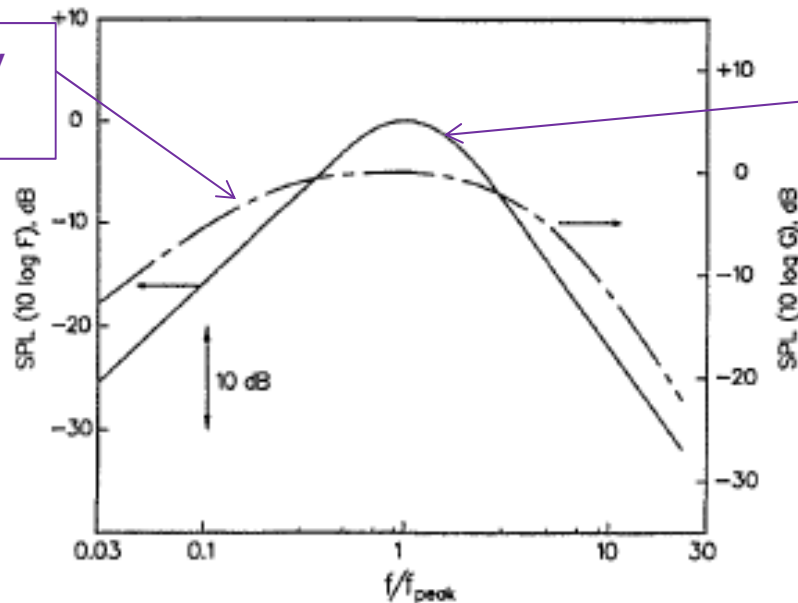


Tam's Two Source Model

- Based on decomposition of measured spectra into two spectral shapes
 - Large Scale Similarity Spectrum
 - Fine Scale Similarity Spectrum
- LSS generated by large scale turbulent structures
- FSS associated from noise from fine-scale turbulence
- Common spectral shapes at both supersonic and subsonic conditions

LSS & FSS Spectra

Fine Scale Similarity (FSS) spectrum



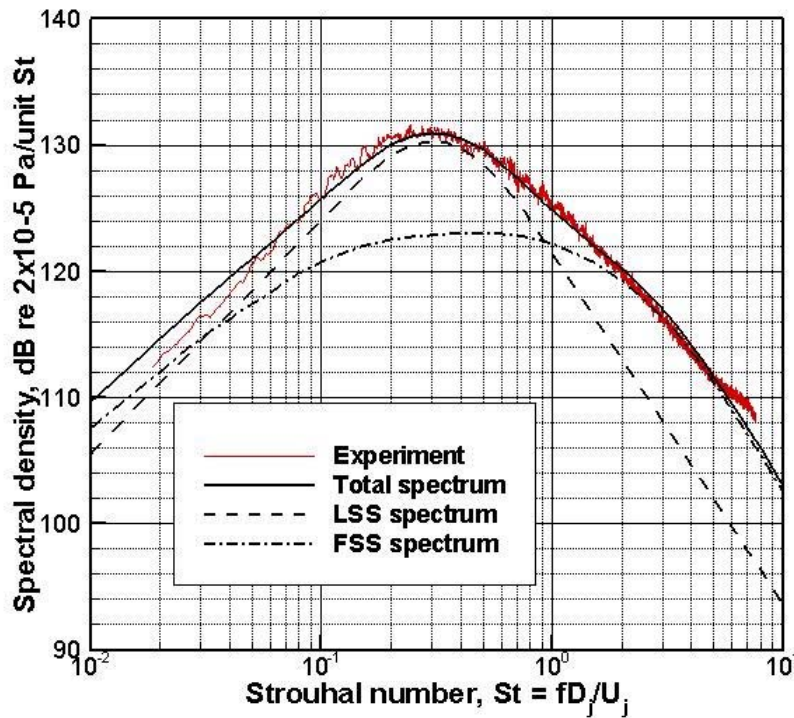
Large Scale Similarity (LSS) spectrum

Figure 2. Similarity spectra for the two components of turbulent mixing noise. — large turbulence structures/ instability waves noise; - - - fine scale turbulence noise.

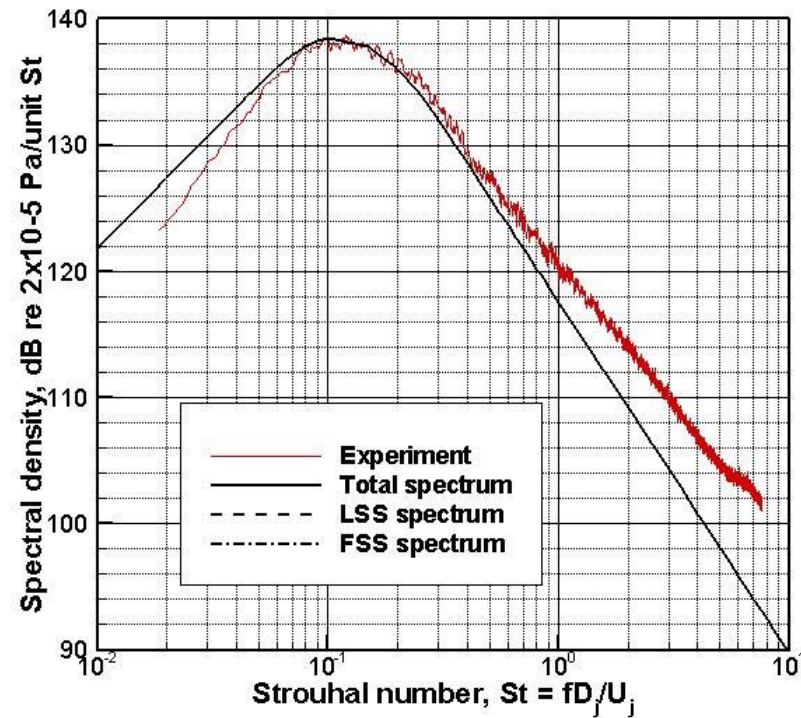
Tam, Golebiowski & Seiner (1996)

Far Field Decomposition

$$M_j = M_d = 1.8, T_r / T_o = 1.648, U_j = 618 \text{ m/s}$$



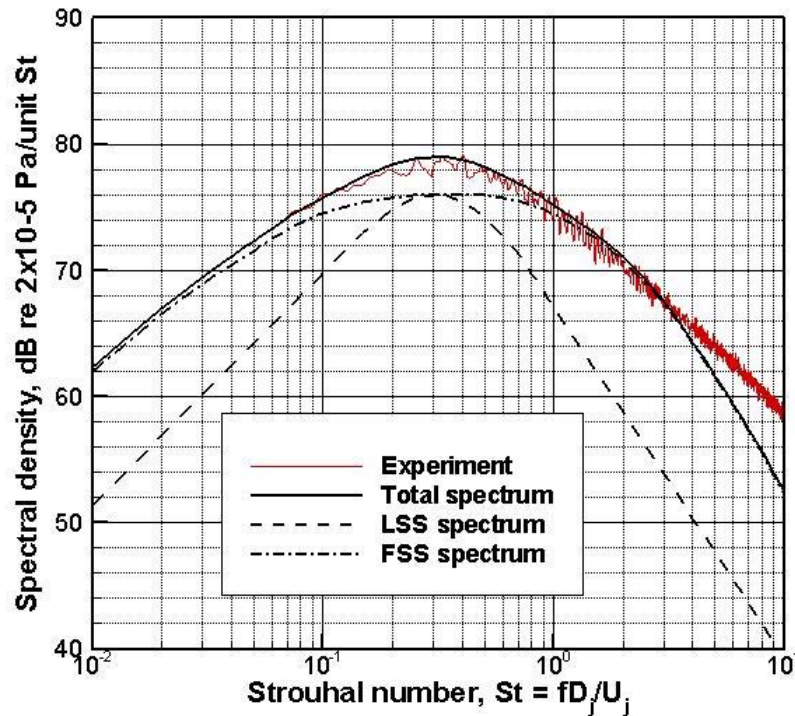
$$\theta = 45^\circ$$



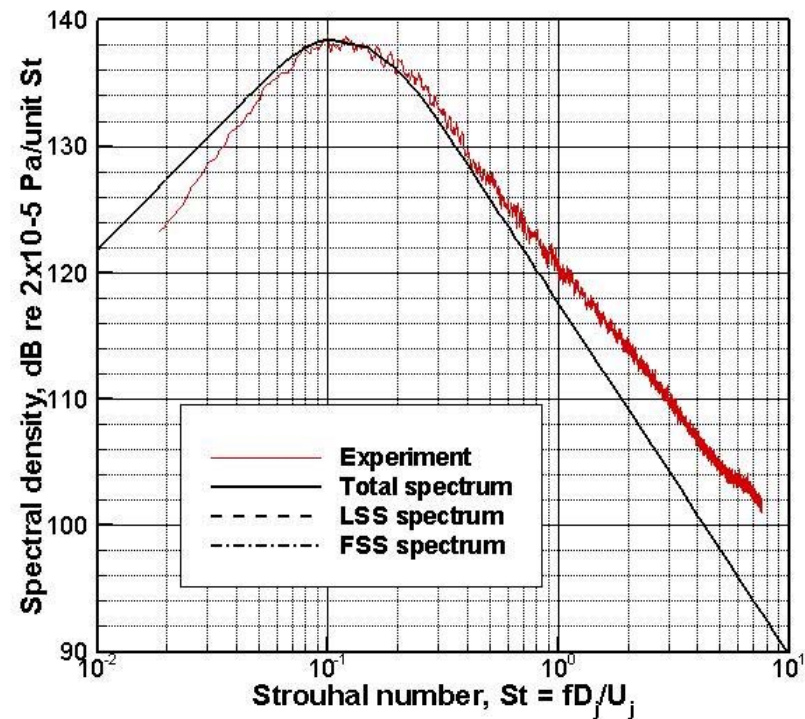
$$\theta = 25^\circ$$

Far Field Decomposition

$$M_j = 0.51, T_r / T_o = 1.0, U_j = 171 \text{ m/s}$$



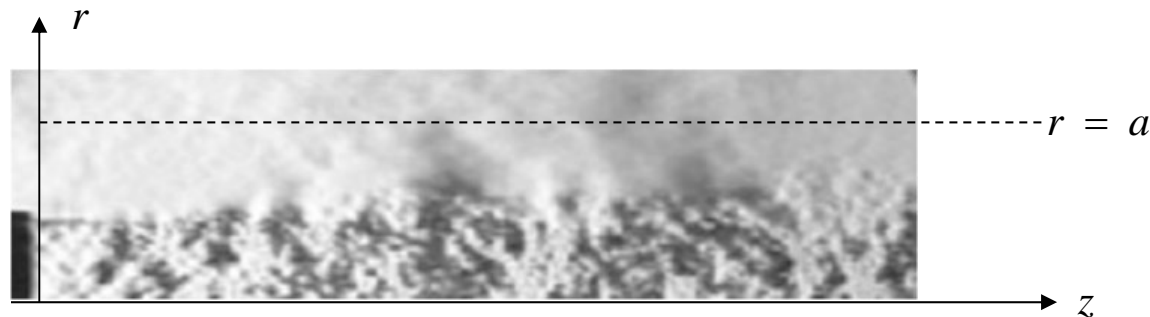
$$\theta = 45^\circ$$



$$\theta = 25^\circ$$

LSS Radiation in Subsonic Jets?

- Only a fraction of the wavenumber content of the LSS energy can radiate
- Remains an efficient mechanism
- Simple model problem:



For $r \geq a$

$$\frac{\partial^2 p}{\partial t^2} - c_o^2 \left(\frac{\partial^2 p}{\partial r^2} + \frac{1}{r} \frac{\partial p}{\partial r} + \frac{1}{r^2} \frac{\partial^2 p}{\partial \phi^2} + \frac{\partial^2 p}{\partial z^2} \right) = 0$$

Simple Model Problem

$$S(r, z, \omega) = \frac{A^2}{2\pi} \rho_j^2 U_j^3 D_j \sum_{n=-\infty}^{\infty} |F_n(r, z, \omega)|^2$$

where,

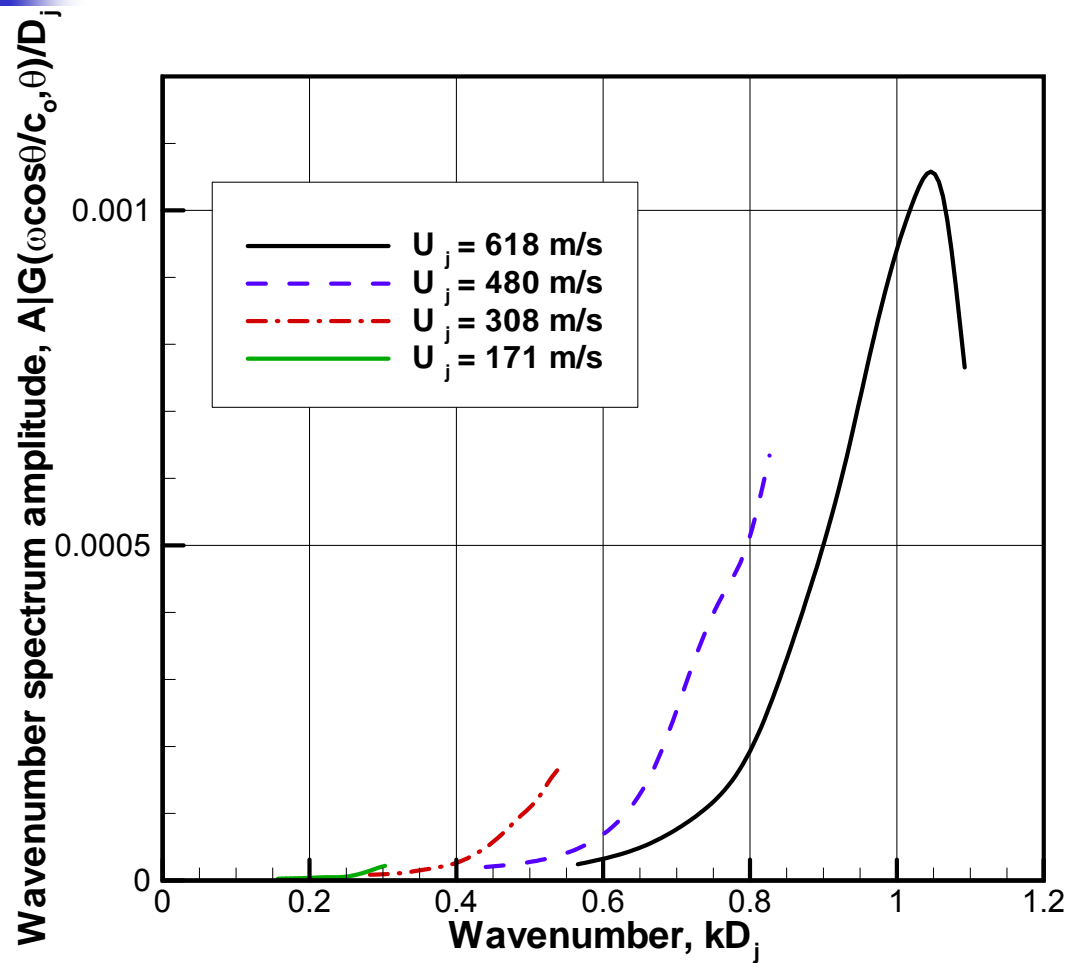
$$F_n(r, z, \omega) = \int_{-\infty}^{\infty} G_n(k, \omega) \frac{H_n^{(1)}(\lambda r)}{H_n^{(1)}(\lambda a)} \exp(ikz) dk$$

In the far field,

$$A^2 \frac{|G_n(\omega \cos \theta / c_o, \omega)|^2}{D_j^2} = \frac{\pi}{2} \left(\frac{R}{D_j} \right)^2 |H_o^{(1)}(\omega a \sin \theta / c_o)|^2 \frac{S(R, \theta, \omega)}{\rho_j^2 U_j^3 D_j}$$

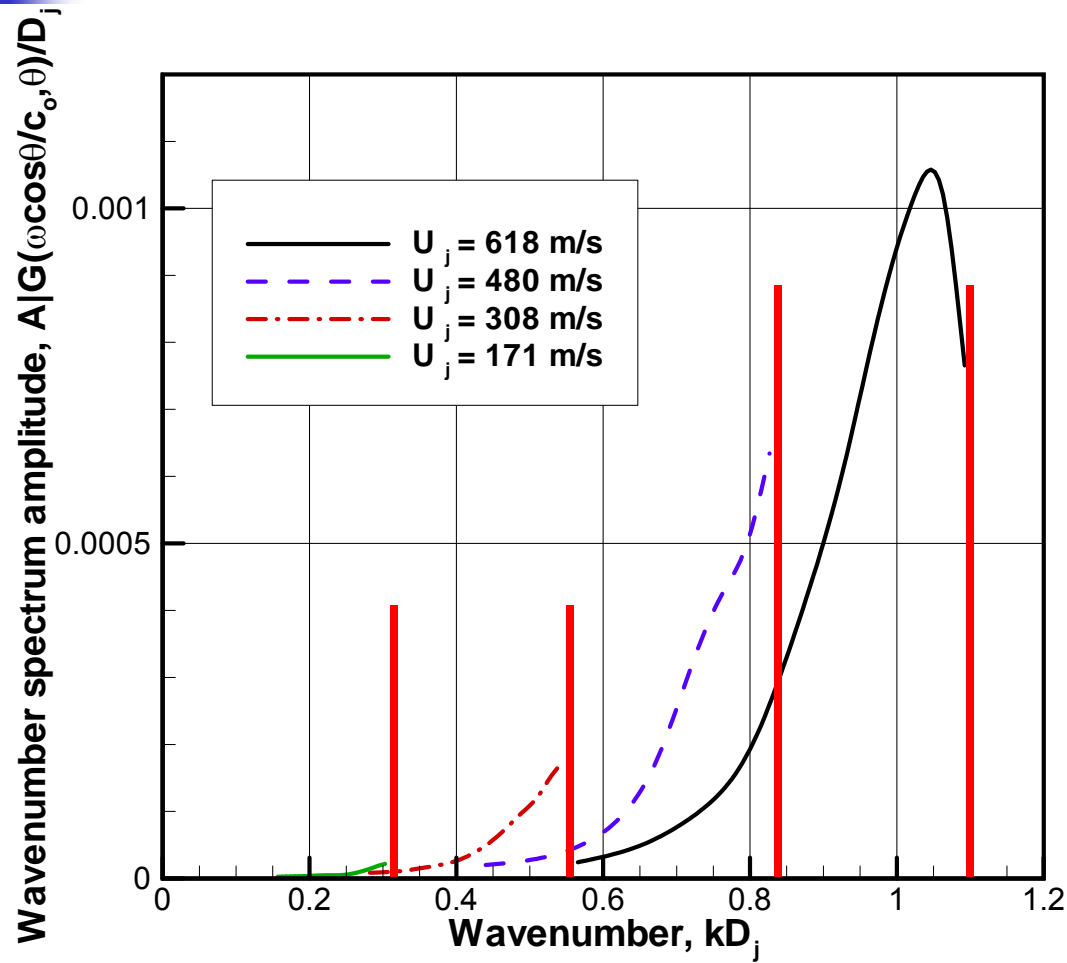
Unknown wavenumber spectrum of LSS

Near Field LSS Wavenumber Spectrum



$St = 0.1$

Near Field LSS Wavenumber Spectrum



$St = 0.1$

$\omega / k = c_o$

Computational Methods

- Significant advances permitted by parallel computations
- “Standard Approach”
 - Unsteady compressible flow simulation using Large Eddy Simulation (LES)
 - Extrapolation from the flow solution to the near and far acoustic fields using permeable surface Ffowcs Williams – Hawking (1969) acoustic analogy

Simulation Strategy (PSU)

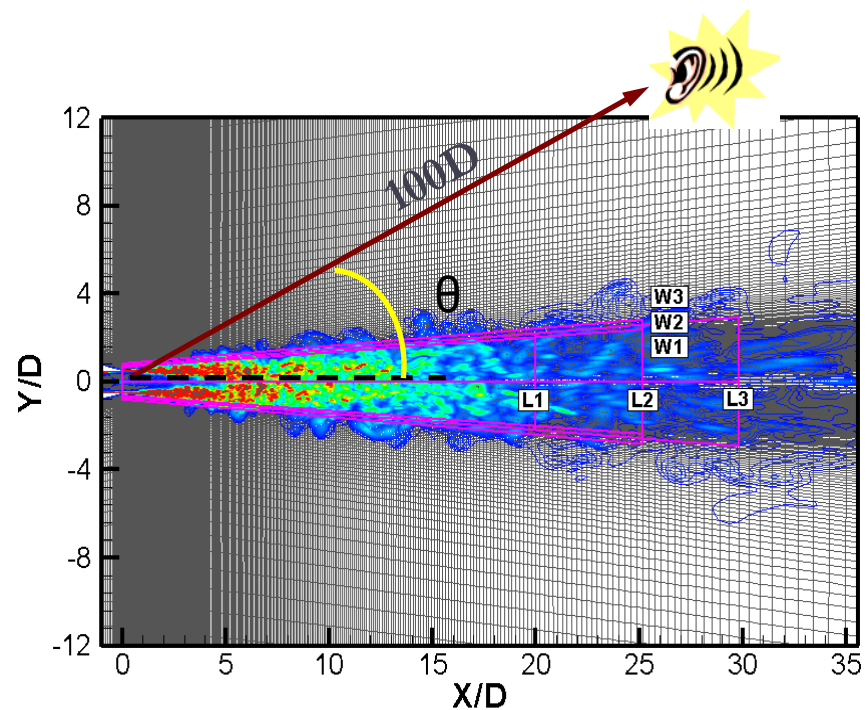
- A hybrid method: CFD + acoustic analogy

Jet flow simulation (CHOPA):

- URANS + modified DES (low dissipation)
- Multi-block structured mesh
- 4th-order DRP
- Parallel computation using MPI
- Dual-time stepping
 - Multigrid
 - Implicit Residual Smoothing (optimized)

Jet noise prediction (PSJFWH):

- FWH equation
- Integrated with the jet flow simulation code



Flow Properties

- Unsteady visualizations

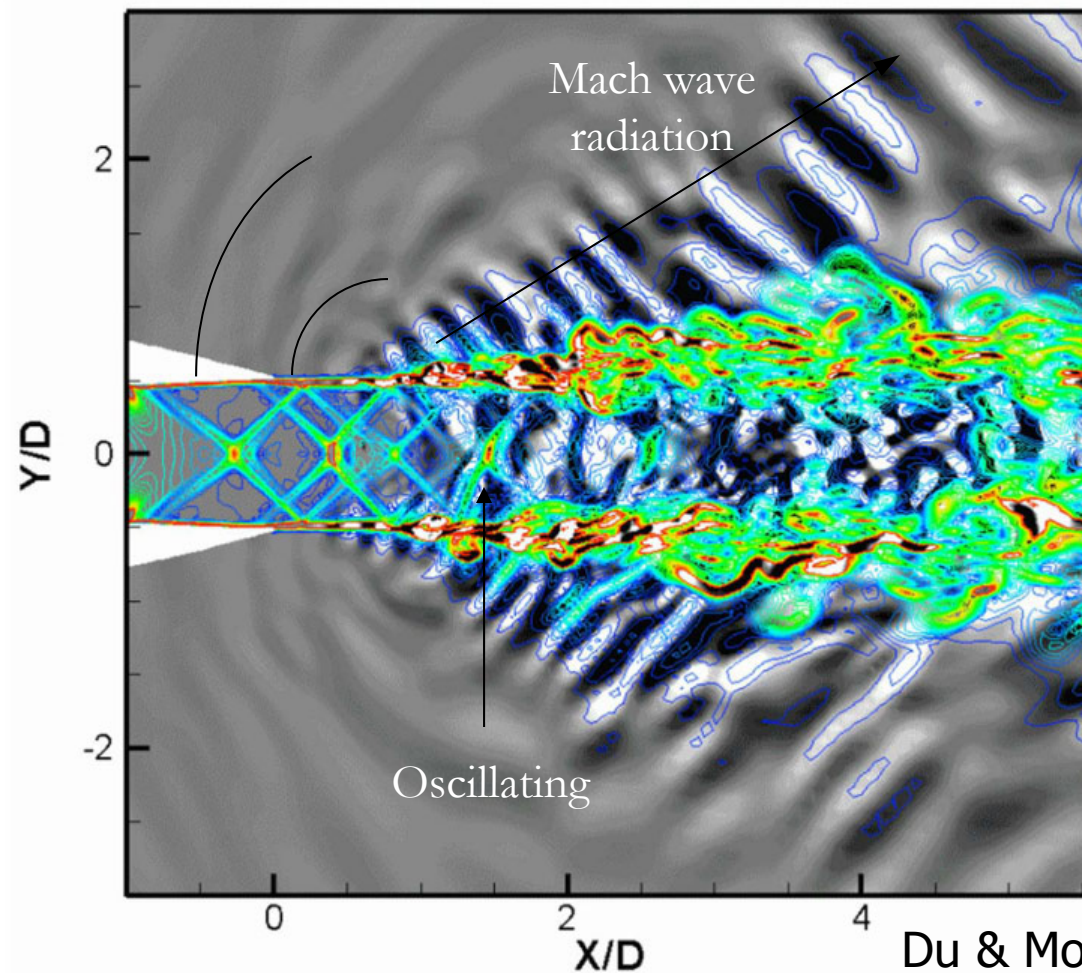
Color contours

Density gradient

Gray background

Pressure time-
derivative

Baseline, $M_j=1.47$
Animation

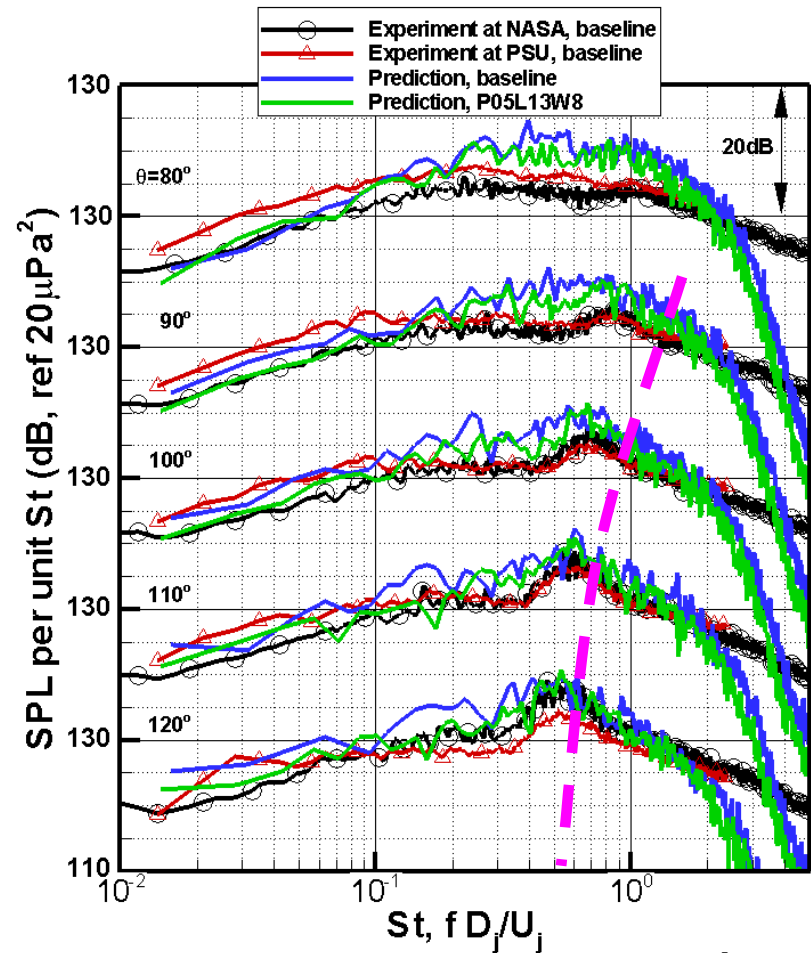
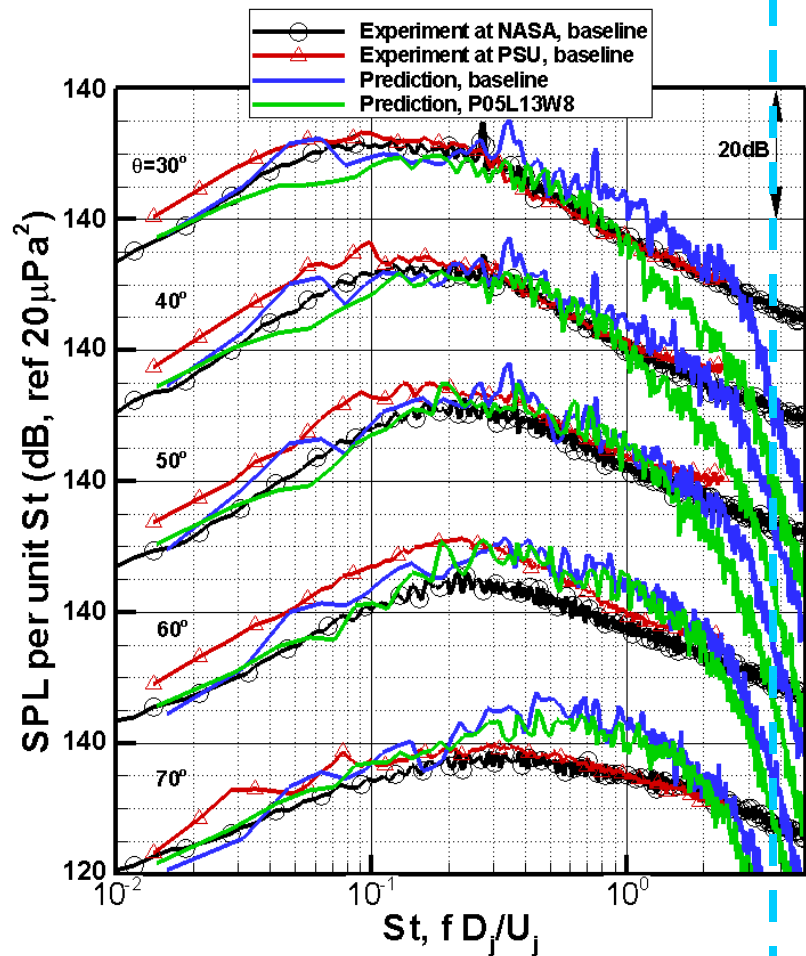


Du & Morris (2011)

Results: Far-field noise

■ Noise spectra: $M_j=1.36$ – $TTR=3.0(?)$

Grid limit, Designed to resolve $St < 4$



Du & Morris (2011)

Noise Reduction

- Separate A8/A9 control
- Three stream VCE
- Thermal shield
- Inverted velocity profile
- Air or water injection
- Chevrons
- Beveled nozzles
- Plasma actuators
- Corrugated seals
- Fluidic inserts

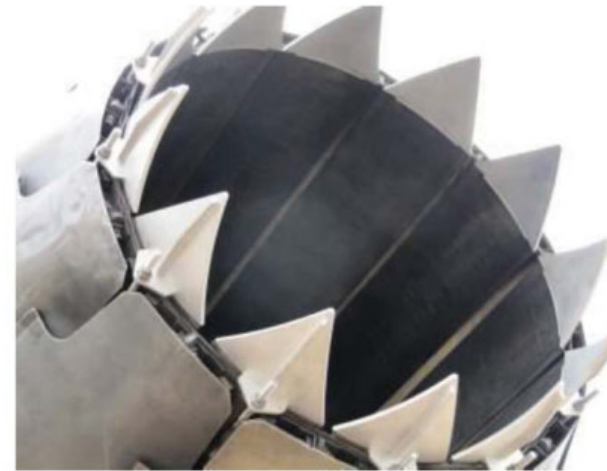
Noise Reduction

- Separate A8/A9 control
- Three stream VCE
- Thermal shield
- Inverted velocity profile
- Air or water injection
- **Chevrons**
- **Beveled nozzles**
- Plasma actuators
- **Corrugated seals**
- **Fluidic inserts**

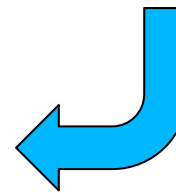
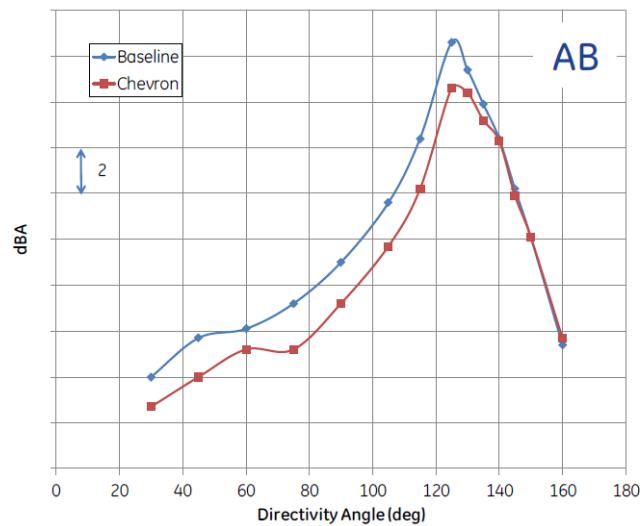
Chevrons



GENx fan chevrons

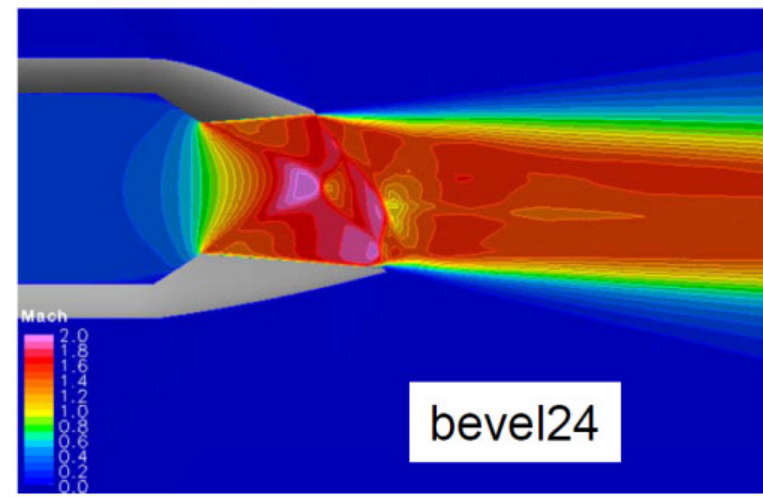
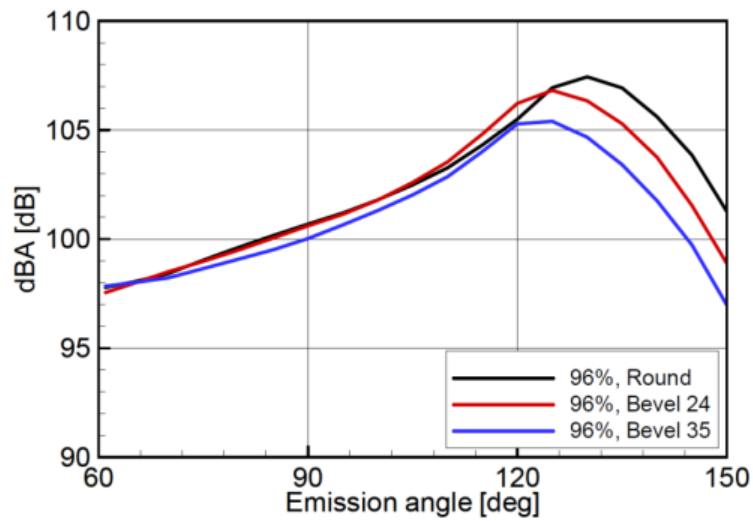
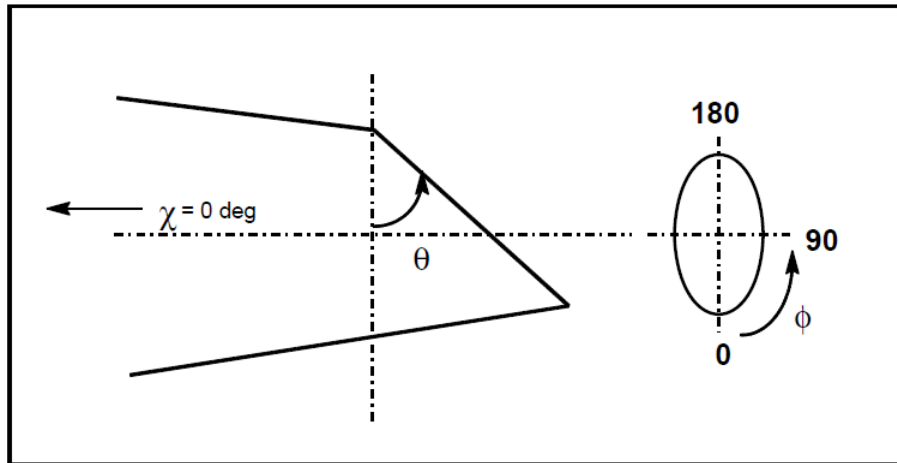


F404 chevrons – static test



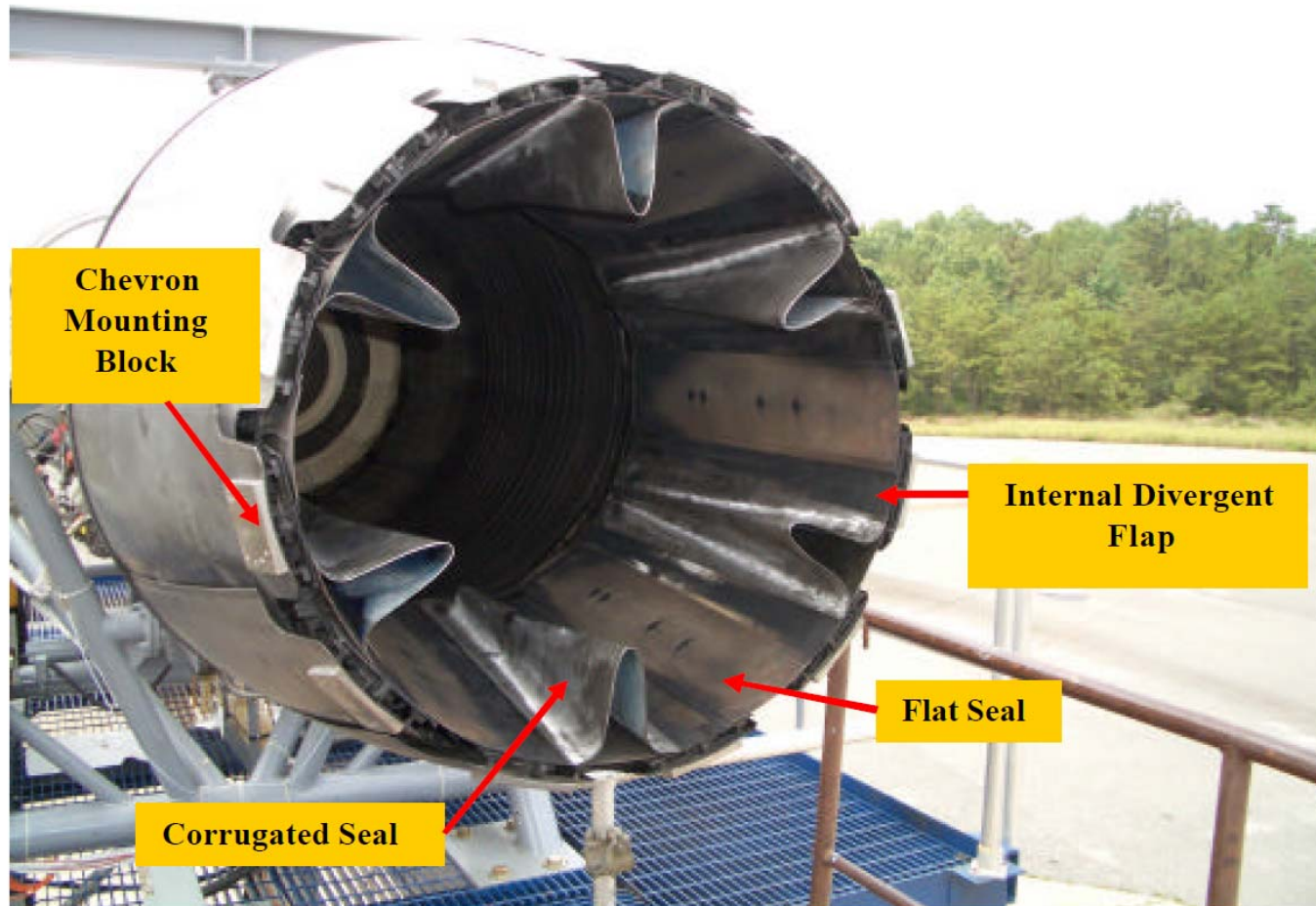
Martens et al. (2011)

Beveled Nozzle



Viswanathan & Czech (2010)

Corrugated Seals

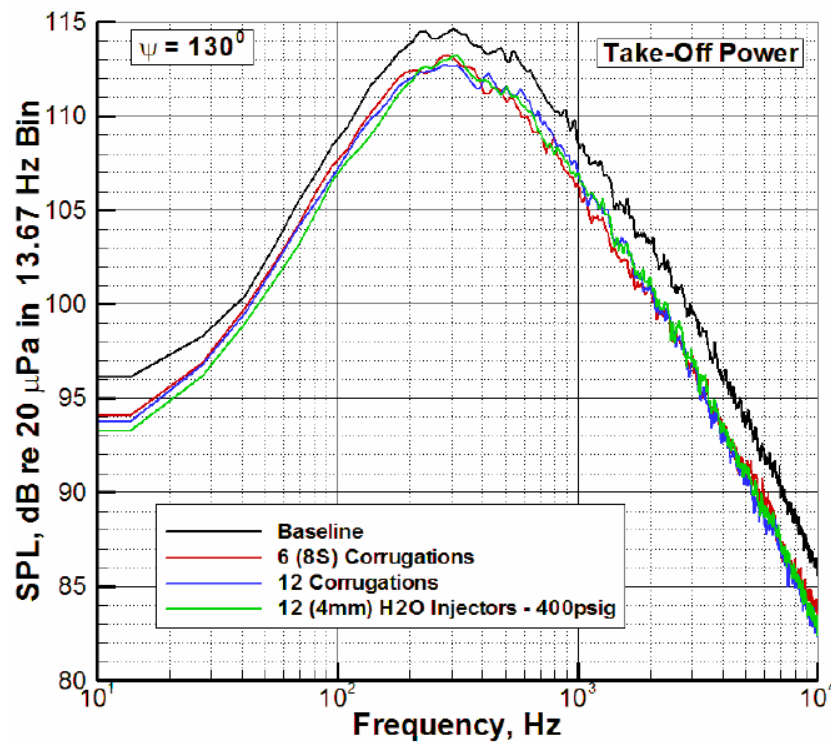


GE F404-400 Static Test

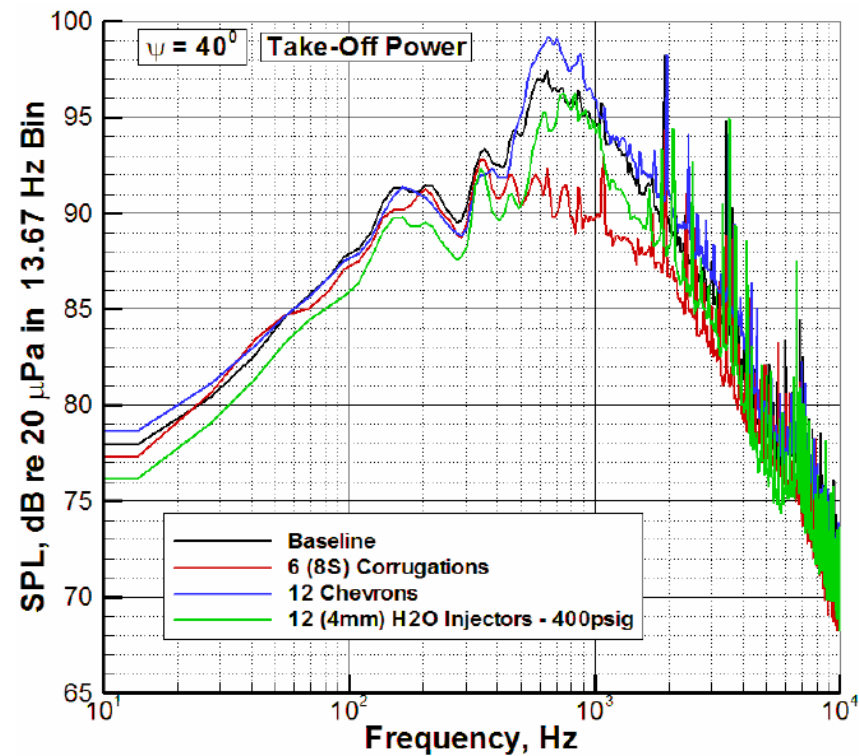
Seiner et al. (2005)

Corrugated Seals

Noise Reduction



Peak noise direction



Upstream direction (BBSAN)

Seiner et al. (2005)

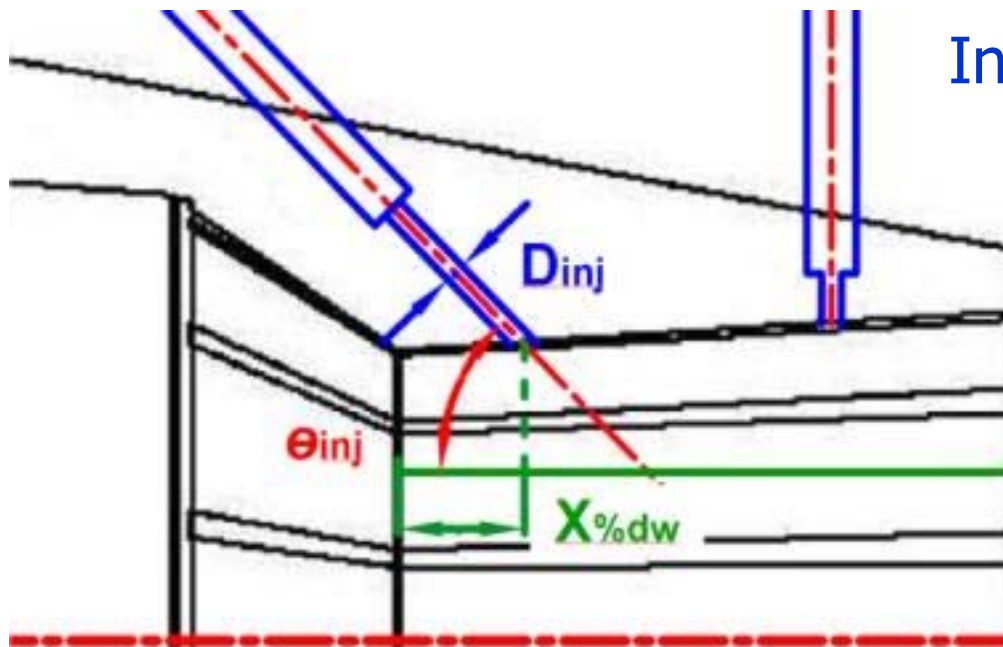
Fluidic Inserts

- Reproduce and enhance benefits of corrugated seals using blowing inside the nozzle
- “Active control”: ability to modify insert shape (or turn off) as engine operating conditions change
- Preliminary tests at model scale
- Comparisons with corrugated seals

Kuo et al. (2012)

Details of the “Fluidic Inserts”

The nozzles are Convergent-Divergent (CD) GE type 404 design with an Area Ratio of 1.295 ($M_d = 1.65$)

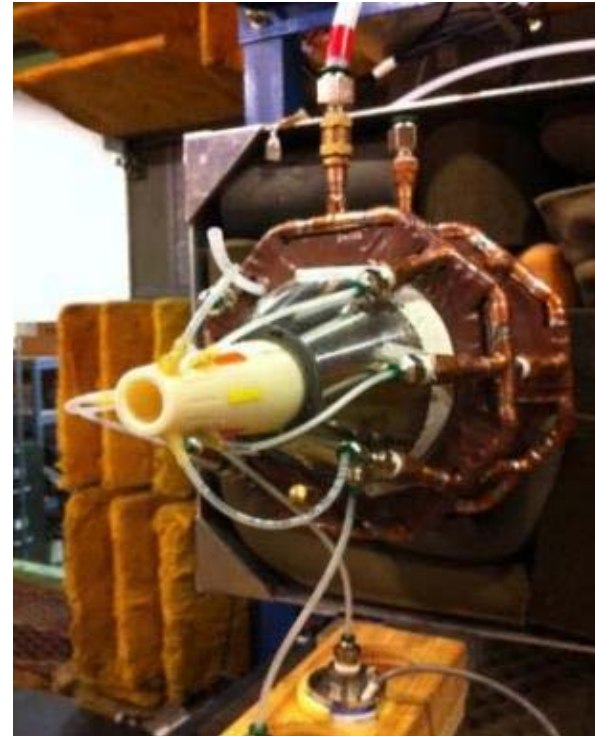
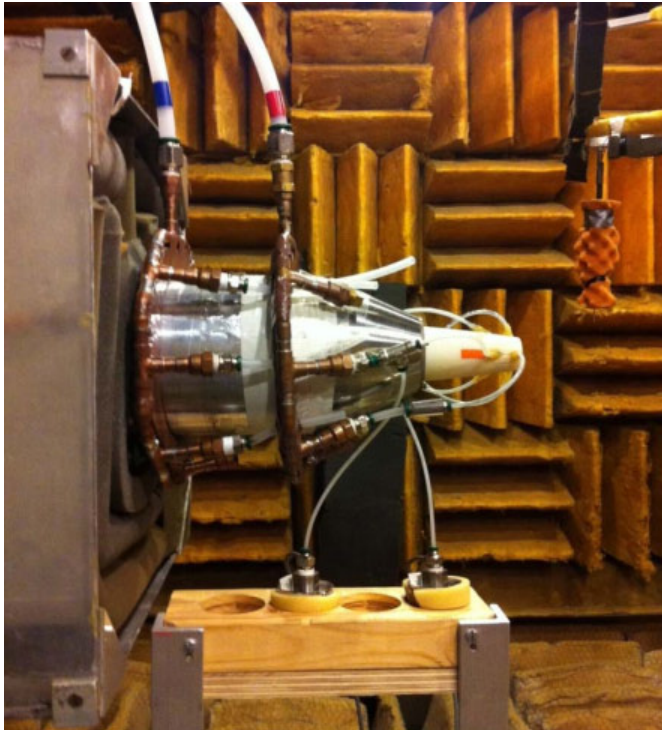


Injection parameters:

- # of injectors
- Injector axial position
- Injector diameter D_{inj}
- Injector angle
- Inlet pressure to injectors

View of Nozzle: 3 Fluidic Inserts – 6 Injectors

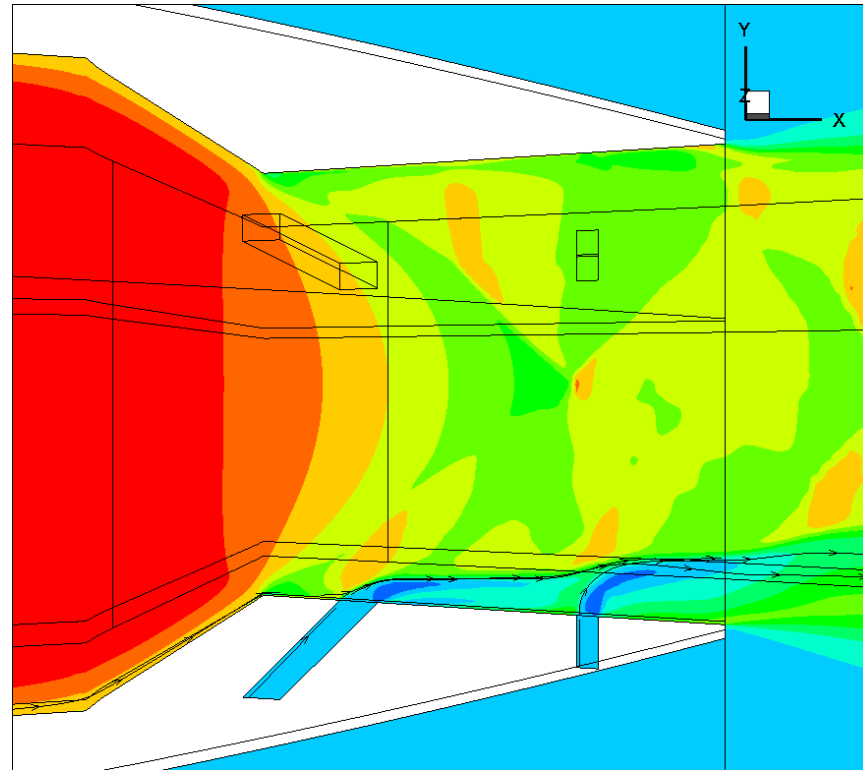
All measurements to date have all injectors from one manifold.



Planned measurements will have all upstream injectors fed from one manifold and the downstream injectors from another.

Data proprietary to Philip J. Morris and Dennis K. McLaughlin. US patent pending

Numerical Simulations



$M_d = 1.65, M_j = 1.36, TTR = 3.0, IPR = 3.0, D_{inj} = 0.06D(1.1mm)$
 6 injectors, 3 fluidic inserts

Data proprietary to Philip J. Morris and Dennis K. McLaughlin. US patent pending

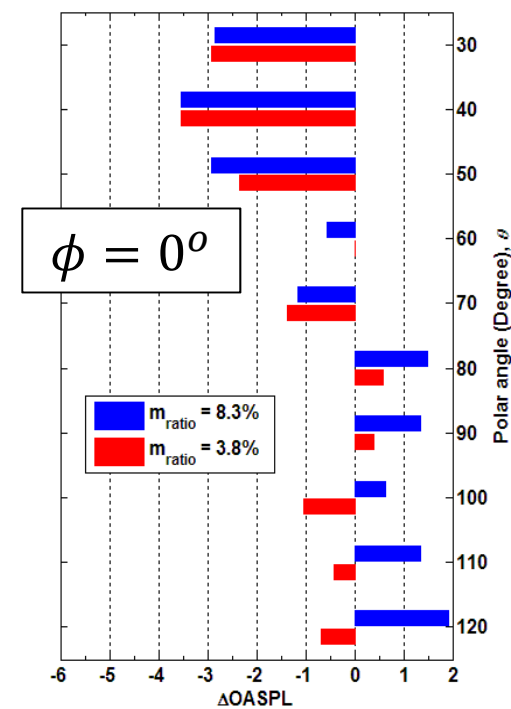
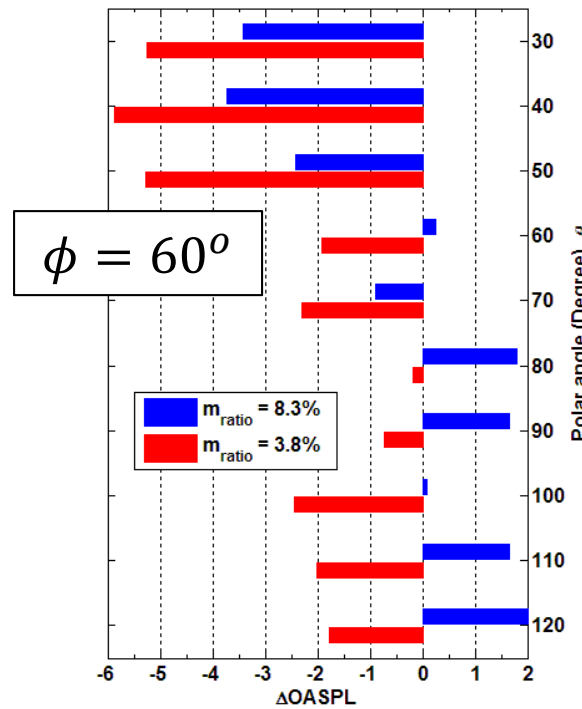
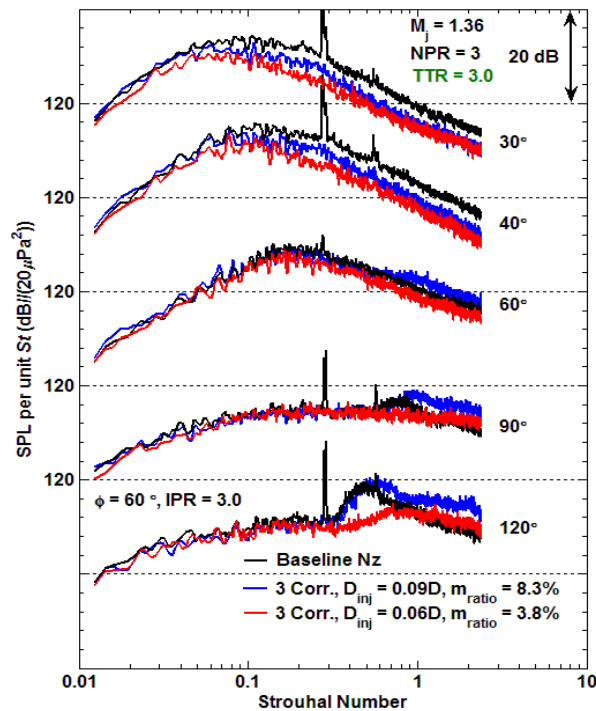
Acoustic Results - 3 Fluidic Inserts

$$M_d = 1.65 \quad M_j = 1.36 \quad TTR = 3.0$$

The best acoustic performance to date achieved with 6 injectors $D_{inj} = 0.06D$ and $m_{ratio} = 3.8\%$ (total)

$$\phi = 60^\circ$$

decrease < OASPL > increase



Lower noise levels at lower injection flow rates

Data proprietary to Philip J. Morris and Dennis K. McLaughlin. US patent pending

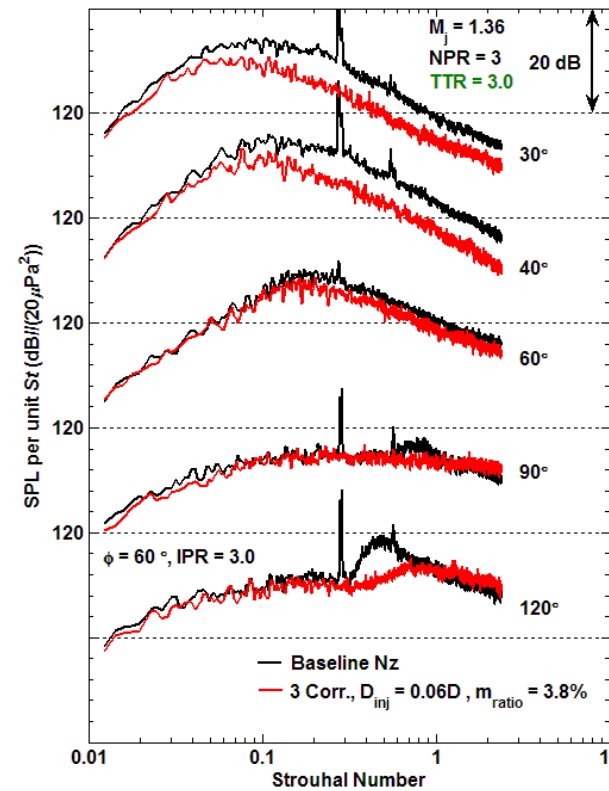
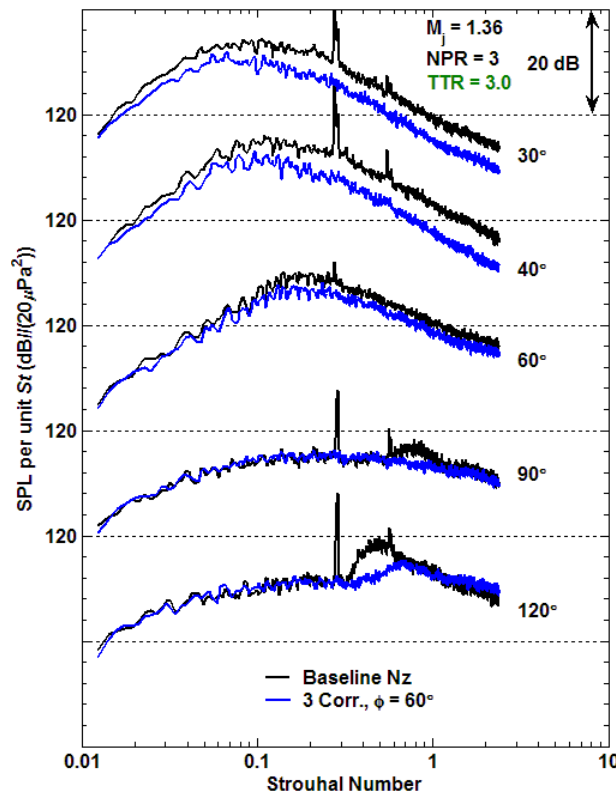
Acoustic Spectra Compared with a Jet with 3 Corrugated Seals

$M_d = 1.65$ $M_j = 1.36$ $TTR = 3.0$

3 "corrugated seals"

3 "fluidic inserts"

$\phi = 60^\circ$



Baseline - no inserts



Future Directions

■ Acoustic analogies:

- Extensions to realistic operating conditions and geometries

■ LSS models:

- Need for first principles model for all operating conditions and geometries

■ Numerical simulations:

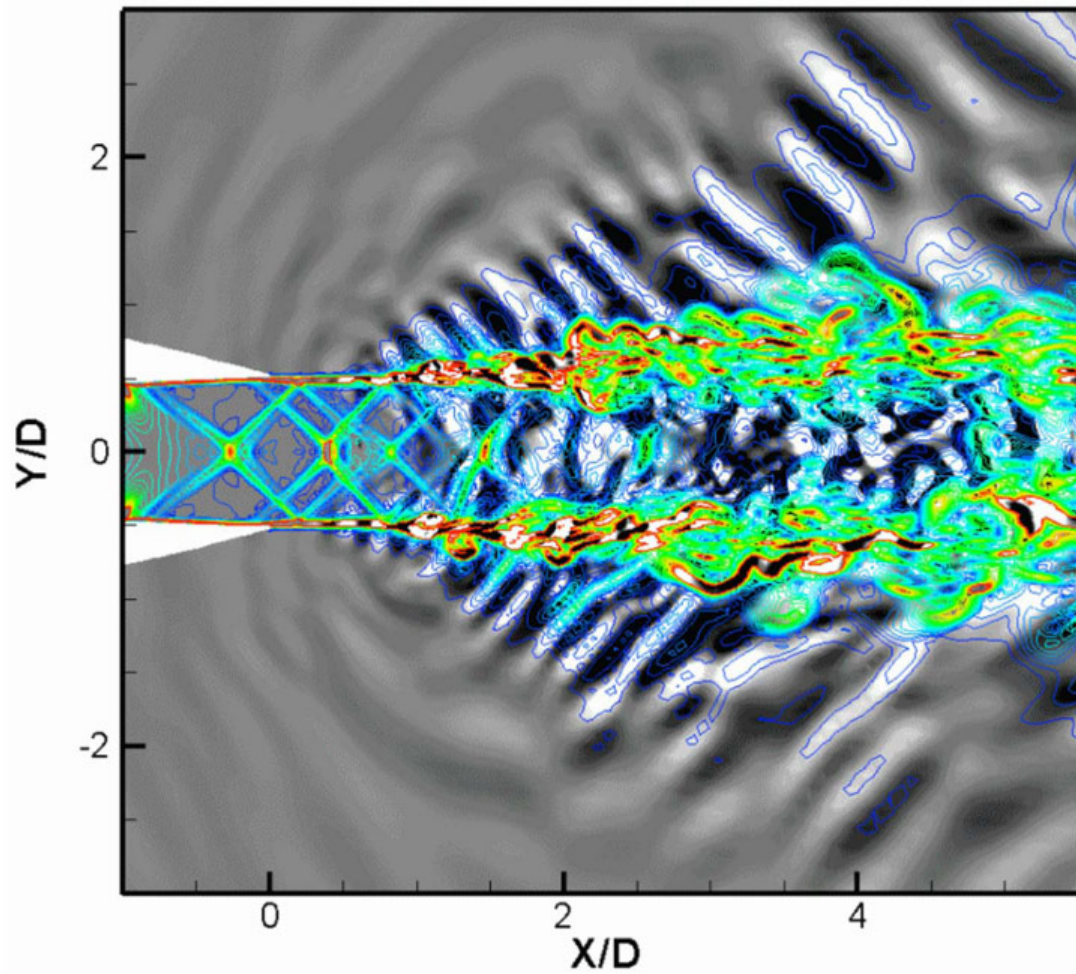
- Extensions to realistic geometries
- Reductions in execution time and increase in frequency range
- Marriage with experimental methods
 - Noise source identification/beamforming
- Inclusion of "real" engine effects
 - Upstream boundary conditions



■ Noise reduction:

- Demonstrations at large scale with forward flight
- Performance testing

Thank you for your attention





References

- A. Dietz, W. Andetta, J. Wilson and G. Passow (2011) "Hearing protection for extreme noise," Paper 3pNS3, 162nd ASA Meeting, San Diego, CA.
- Veterans Benefits Administration (2011) "Annual Benefits Report FY 2011," www.vba.va.gov/REPORTS/abr/2011.abr.pdf. Last accessed 8/15/12.
- K. Viswanathan (2004) "Aeroacoustics of hot jets," *J. Fluid Mech.*, **516**, 39-82.
- K. Viswanathan (2006) "Scaling laws and a method for identifying components of jet noise," *AIAA Journal*, **44**(10), 2274-2285.
- M. Lighthill (1952, 1954) "On sound generated aerodynamically. Part I: General theory. Part II: Turbulence as a source of sound," *Proc. Roy. Soc. Lond.*, **A211**, 564-587, **A222**, 1-32.
- J. Ffowcs Williams (1963) "The noise from turbulence convected at high speed," *Phil. Trans. Roy. Soc.*, **255**, 469-503.
- P. Lush (1971) "Measurements of jet noise and comparison with theory," *J. Fluid Mech.*, **46**, 477-500.
- G. Lilley (1974) "On the noise from jets," in Noise Mechanisms, AGARD CP-131, 13.1-13.12.
- R. Mani (1976) "The influence of flow on jet noise," *J. Fluid Mech.*, **80**, 753-793.
- J. Bridges (2008) "State of jet noise predictions – NASA perspective," Fundamental Aeronautics Program Annual Meeting, Atlanta, GA.
- M. Goldstein and S. Leib (2008) "The aeroacoustics of slowly diverging supersonic jets," *J. Fluid Mech.*, **600**, 291-337.
- S. Karabasov et al. (2010) "Jet noise: acoustic analogy informed by Large Eddy Simulation," *AIAA Journal*, **48**(9), 1312-1325.
- M. Harper-Bourne and M. Fisher (1974) "The noise from shock waves in supersonic jets," in Noise Mechanisms, AGARD CP-131, 11.1-11.13.



References

- C. Tam (1987) "Stochastic model theory of broadband shock-associated noise from supersonic jets," *J. Sound Vib.*, **116**, 265-302.
- P. Morris and S. Miller (2010) "Prediction of broadband shock-associated noise using RANS-CFD," *AIAA Journal*, **48**(12), 2931-2944.
- G. Brown and A. Roshko (1974) "On density effects and large structure in turbulent mixing layers," *J. Fluid Mech.*, **64**, 775-816.
- J. Lepicovsky et al. (1986) "Acoustic control of free jet mixing," *J. Prop. Power*, **2**(4), 323-330.
- C. Tam, M. Golebiowski and J. Seiner (1996) "On the two components of turbulent mixing noise from supersonic jets," AIAA Paper 96-1716.
- P. Morris (2009) "A note on noise generation by large scale turbulent structures in subsonic and supersonic jets," *Int. J. Aeroacoustics*, **8**(4), 301-315.
- J. Ffowcs Williams and D. Hawkings (1969) "Sound generation by turbulence and surfaces in motion," *Phil. Trans. Roy. Soc.*, **264**, 321-342.
- Y. Du and P. Morris (2011) "Noise simulations of supersonic jets for chevron nozzles," AIAA Paper 2011-2787.
- S. Martens, J. Spyropoulos and Z. Nagel (2011) "The effect of chevrons on crackle – engine and model scale results," GT2011-46417, ASME Turbo Expo 2011, Vancouver, BC.
- K. Viswanathan and M. Czech (2010) "Adaptation of the beveled nozzle for high speed jet noise reduction," AIAA Paper 2010-654.
- J. Seiner, L. Ukeiley and B. Jansen (2005) "Aero-performance efficient noise reduction for the F404-400 engine," AIAA Paper 2005-3048.
- C.-W. Kuo, P. Morris and D. McLaughlin (2012) "Noise reduction in supersonic jets by nozzle fluidic inserts," AIAA Paper 2012-2210.